Sustained Virological Response Reduces Incidence of Onset of Type 2 Diabetes in Chronic Hepatitis C

Yasuji Arase, Fumitaka Suzuki, Yoshiyuki Suzuki, Norio Akuta, Masahiro Kobayashi, Yusuke Kawamura, Hiromi Yatsuji, Hitomi Sezaki, Tetsuya Hosaka, Miharu Hirakawa, Kenji Ikeda, and Hiromitsu Kumada

Diabetes is present in patients with chronic hepatitis C virus infection. The aim of this retrospective cohort study was to assess the cumulative development incidence and predictive factors for type 2 diabetes after the termination of interferon therapy in Japanese patients positive for hepatitis C virus (HCV). A total of 2,842 HCV-positive patients treated with interferon (IFN) monotherapy or combination therapy with IFN and ribavirin were enrolled. The mean observation period was 6.4 years. An overnight (12-hour) fasting blood sample or a casual blood sample was taken for routine analyses during follow-up. The primary goal was the onset of type 2 diabetes. Evaluation was performed by using the Kaplan-Meier method and Cox proportional hazard analysis. Of 2,842 HCV patients, 143 patients developed type 2 diabetes. The cumulative development rate of type 2 diabetes was 3.6% at 5 years, 8.0% at 10 years, and 17.0% at 15 years. Multivariate Cox proportional hazard analysis revealed that type 2 diabetes development after the termination of IFN therapy occurred when histological staging was advanced (hazard ratio 3.30; 95% confidence interval [CI] 2.06-5.28; $P < 0.001$), sustained virological response was not achieved (hazard ratio 2.73; 95% CI 1.77-4.20; $P < 0.001$), the patient had pre-diabetes (hazard ratio 2.19; 95% CI 1.43-3.37; $P < 0.001$), and age was ≥50 years (hazard ratio 2.10; 95% CI 1.38-3.18; $P < 0.001$). *Conclusion:* Our results indicate sustained virological response causes a two-thirds reduction in the risk of type 2 diabetes development in HCV-positive patients treated with IFN. (HEPATOLOGY 2009;49:000-000.)

Hepatitis C virus (HCV) is one of the more common causes of chronic liver disease in world. Chronic hepatitis C is an insidiously progressive form of liver disease that relentlessly but silently progresses to cirrhosis in 20% to 50% of cases over a period of 10 to 30 years.[1-3] In addition, HCV is a major risk for hepatocellular carcinoma (HCC).[4-8] Moreover, chronic HCV infection has been associated with a variety of extrahepatic complications such as essential mixed cryoglobulinemia, porphyria cutanea tarda, membranoproliferative glomerulonephritis, autoimmune thyroiditis, sialadenitis, and cardiomyopathy.[9-13] Lately, data supporting a link between type 2 diabetes mellitus (T2DM) and chronic hepatitis C infection have been reported.[14,15]

Although there is growing evidence to support the concept that HCV infection is a risk factor for developing T2DM, there have been a few interventional studies confirming this issue. This issue needs to be confirmed with a long-term follow-up of patients with high risk of developing diabetes. Thus, prospective studies including metabolic evaluations are clearly needed to clarify these issues.

With this background in mind, the cohort study was initiated to investigate the cumulative incidence and risk factors of T2DM after prolonged follow-up in HCV-infected patients treated with interferon (IFN) monotherapy or combination therapy with IFN and ribavirin. The strengths of the current study are the large numbers of patients included and the long-term follow-up of patients.

Patients and Methods

Patients. There were 5,890 patients diagnosed with chronic HCV infection and treated with IFN mono-

Abbreviations: CI, confidence interval; FPG, fasting plasma glucose; HCC, hepatocellular carcinoma; HCV, hepatitis C virus; IFN, interferon; SVR, sustained virological response; T2DM, type 2 diabetes mellitus.

From the Department of Hepatology, Toranomon Hospital, Tokyo, Japan.

Received September 25, 2008; accepted October 13, 2008.

Supported in part by grants-in-aid from Okinaka Memorial Institute for Medical Research and the Japanese Ministry of Health, Labor, and Welfare.

Address reprint requests to: Yasuji Arase, M.D., Department of Hepatology, Toranomon Hospital, 2-2-2, Toranomon, Minato-ku, Tokyo 105-8470, Japan. E-mail: es9y-ars@asahi-net.or.jp; fax: (81)-3-3582-7068.

Published online in Wiley InterScience (www.interscience.wiley.com).

DOI 10.1002/hep.22703

Potential conflict of interest: Nothing to report.

therapy or combination IFN + ribavirin therapy between September 1990 and March 2007 in the Department of Hepatology, Toranomon Hospital, Tokyo, Japan. Of these, 2,842 patients satisfied the following criteria: (1) no evidence of diabetes mellitus for 3 months after the termination of IFN (plasma glucose concentration <126 mg/dL [6.9 mmol/L] in the fasting state, <200 mg/dL [11.0 mmol/L] in casual state and/or 2 hours after a 75-g oral glucose load); (2) features of chronic hepatitis or cirrhosis diagnosed via laparoscopy and/or liver biopsy before the initiation of IFN therapy; (3) positivity for serum HCV RNA before the initiation of IFN therapy; (4) period of ≤1 year of IFN therapy; (5) negativity for hepatitis B surface antigen (HBsAg), antinuclear antibodies, or antimitochondrial antibodies in serum, as determined via radioimmunoassay or spot hybridization; (6) no evidence of HCC nodules as shown on ultrasonography and/or computed tomography; and (7) no underlying systemic disease, such as systemic lupus erythmatosus or rheumatic arthritis.

Patients who were taking medications known to alter glucose tolerance or had illnesses that could seriously reduce their life expectancy or their ability to participate in the trial were excluded from the study. Patients were classified as having normal glucose or pre-diabetes based on fasting plasma glucose (FPG), casual plasma glucose, or 2-hour plasma glucose. The normal glucose group was regarded as having an FPG of <100 mg/dL, casual plasma glucose of <140 mg/dL, and/or 2-hour plasma glucose of <140 mg/dL. The pre-diabetes group was regarded as having an FPG of 100-125 mg/dL, casual plasma glucose of 140-200 mg/dL, and/or 2-hour plasma glucose of 140-200 mg/dL.[16]

Next, we assessed predictive factors for T2DM in chronic hepatitis C patients treated with IFN. The physicians in charge explained the purpose and method of this clinical trial to each patient and/or the patient's family. Informed consent was obtained from all living patients included in the present cohort study. The study was approved by the Institutional Review Board of our hospital.

Outcome Measures. The primary outcome was T2DM, diagnosed by the use of the 2003 criteria of the American Diabetes Association.[16] These criteria include (1) casual plasma glucose ≥200 mg/dL; (2) FPG ≥126 mg/dL; (3) 2-hour post-glucose (oral glucose tolerance test) ≥200 mg/dL.

Laboratory Investigation. Anti-HCV was detected using a second-generation enzyme-linked immunosorbent assay (ELISA II; Abbott Laboratories, North Chicago, IL). HCV-RNA was determined by the Amplicor method (Cobas Amplicor HCV Monitor Test, version 2.0; Roche, Tokyo, Japan). Hepatitis B surface antigen was tested via radioimmunoassay (Abbott Laboratories, Detroit, MI). The used serum samples were stored at −80°C at the first consultation. Diagnosis of HCV infection was based on detection of serum HCV antibody and positive RNA. Height and weight were recorded at baseline, and the body mass index was calculated as weight (in kg)/height (in m^2).

Evaluation of Liver Cirrhosis. Liver status of the 2,842 patients was mainly determined via peritoneoscopy and/or liver biopsy. Liver biopsy specimens were obtained using a modified Vim Silverman needle with an internal diameter of 2 mm (Tohoku University, Kakinuma Factory, Tokyo, Japan), fixed in 10% formalin, and stained with hematoxylin-eosin, Masson's trichrome, silver impregnation, and periodic acid-Schiff after diastase digestion. The size of specimens for examination was more than six portal areas.[17]

Follow-up. The starting time of follow-up was 3 months after the termination of IFN therapy. After that, patients were followed up monthly to tri-monthly in our hospital. Physical examination and biochemical tests were conducted at each examination together with regular check-up. An overnight (12-hour) fasting blood sample or a casual blood sample was taken for routine analyses. These included aminotransferase activities, total cholesterol, platelet counts, and serum HCV RNA level. Three hundred twenty-four patients were lost to follow-up; because the appearance of T2DM and death was not identified in these patients, they were considered as censored data in the statistical analysis.[18] Moreover, patients retreated with antiviral agents were regarded as withdrawals at the time of starting the retreatment of antiviral agents.

Statistical Analysis. The cumulative appearance rate of T2DM was calculated from 3 months after the termination of IFN treatment to the appearance of T2DM using the Kaplan-Meier method. Differences in the development of T2DM were tested using the log rank test. Independent factors associated with the incidence rate of T2DM were analyzed by the Cox proportional hazard model. The following 11 variables were analyzed for potential covariates for incidence of T2DM at the time of termination of IFN therapy at our hospital: age, sex, state of liver disease (chronic hepatitis or liver cirrhosis), body mass index, glucose level, aspartate aminotransferase level, alanine aminotransferase level, type of IFN, total dose of IFN, efficacy of IFN therapy, hypertension, triglyceride level, and total cholesterol level. A P value of less than 0.05 was considered significant. Data analysis was performed using SPSS 11.5 for Windows (SPSS, Chicago, IL).

Results

Patient Characteristics. Table 1 shows the characteristics of the 2,842 HCV-positive patients treated with

Table 1. Patient Characteristics

N	2,842
Sex (male/female)	1,778/1,064
Age (years)	51.8 ± 9.0
Height (cm)	163.8 ± 9.1
Body weight (kg)	62.7 ± 11.7
Body mass index	23.3 ± 3.2
Blood pressure (systolic/diastolic, mm Hg)	128 ± 18/77 ± 12
HCV genotype (1b/2a/2b/other)	744/752/290/56
HCV RNA level (KIU/mL)	593 ± 540
Staging (non-LC/LC)	2,649/193
Blood glucose level (normal/prediabetes)	2,601/241
Fasting plasma glucose (mg/dL)	87 ± 24
Triglyceride (mg/dL)	166 ± 31
Total bilirubin (g/dL)	102 ± 56
AST (IU/L)	74 ± 63
ALT (IU/L)	116 ± 102
IFN monotherapy*/combination therapy†	2,417/425
Efficacy of treatment (SVR/non-SVR)	1,175/1,667
Follow-up period (years)	6.4 ± 5.0

Data are expressed as the number of patients or mean ± standard deviation.

Abbreviations: ALT, alanine aminotransferase; AST, aspartate aminotransferase; LC, liver cirrhosis; SVR, sustained virological response.

*Outbreak of IFN monotherapy: recombinant IFN-α2a, 304 cases; recombinant IFN-α2b, 235 cases; natural IFN-bα, 1,355 cases; natural IFN-β, 522 cases; total dose of IFN = 598 ± 170 MU.

†Outbreak of combination therapy: recombinant IFN-α2b + ribavirin, 175 cases; total dose of IFN = 537 ± 196 MU; total dose of ribavirin = 182 ± 69 g; pegylated IFN-α2b + ribavirin, 250 cases; total dose of pegylated IFN = 4.28 ± 1.17 mg; total dose of ribavirin = 232 ± 60 g.

IFN monotherapy or combination therapy with IFN and ribavirin. The sustained virological response (SVR) rate was 36.7% (886/2417) in IFN monotherapy and 68% (289/425) in IFN + ribavirin therapy. Thus, the number of patients with SVR was 1,175. The mean period after the termination of antiviral drugs was 6.4 years.

Incidence of T2DM in Patients with HCV. A total of 143 patients (102 men and 41 women) developed T2DM during a mean observation period of 6.4 years. Of these, 26 were SVR and 117 were non-SVR. The cumulative development rate of T2DM was determined to be 3.6% at 5 years, 8.0% at 10 years, and 17.0% at 15 years using the Kaplan-Meier method (Fig. 1). The factors associated with the incidence of T2DM in all 2,842 patients treated with IFN therapy are shown in Table 2.

Multivariate Cox proportional hazard analysis revealed that type 2 diabetes development after the termination of IFN therapy occurred when histological staging was advanced (hazard ratio 3.30; 95% confidence interval [CI] 2.06-5.28; $P < 0.001$), sustained virological response was not achieved (hazard ratio 2.73; 95% CI 1.77-4.20; $P < 0.001$), patient had pre-diabetes (hazard ratio 2.19; 95% CI 1.43-3.37; $P < 0.001$), and age was >50 years (hazard ratio 2.10; 95% CI 1.38-3.18; $P < 0.001$). SVR causes a two-thirds reduction of development of T2DM in patients treated with IFN. In addition to SVR, age ≥50 years, liver cirrhosis, and pre-diabetes contribute to a high risk of developing diabetes. The cumulative development rates of T2DM based on difference of age, efficacy of the IFN therapy, histological diagnosis, and glucose level at the starting time of follow-up are shown in Fig. 2.

Fig. 3 shows the impact of reduction due to SVR on the incidence of T2DM in patients with ≥50 years, liver cirrhosis, or pre-diabetes. When patients with age ≥50 years, liver cirrhosis, and pre-diabetes have SVR after IFN therapy, SVR could statistically reduce the onset of T2DM compared with those without SVR.

Discussion

We have described the development incidence of diabetes after the termination of antiviral therapy in HCV-positive patients treated with IFN therapy in the present study. Diabetes has been reported in less than 0.08% of patients treated with IFN[19,20]; thus, to exclude diabetes originating from IFN-related side effects, patients without diabetes for 3 months after the termination of IFN were enrolled in the present study. The present study indicates that the annual incidence of T2DM for a prolonged follow-up after the termination of IFN therapy among HCV patients is 0.8% to 1.0%. The present study was limited by a retrospective cohort trial. We started the present study in 1991 based on the diabetes mellitus criteria published by Fajans.[21] However, after that, diabetes mellitus criteria were revised. We thus rechecked the diagnosis of T2DM based on the diabetes mellitus criteria of 2003 in patients seen prior to 2003.[16] Because of rechecking the diagnosis of T2DM on the basis of diabetes mellitus criteria in 2003, the present study was regarded as a retrospective cohort study. However, the patients were

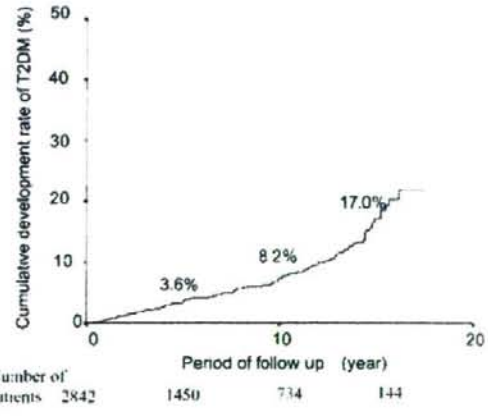

Fig. 1. Cumulative development rate of T2DM in patients treated with IFN.

Table 2. Predictive Factors for T2DM Development

Variables	Univariate Analysis		Cox Regression	
	HR (95% CI)	P Value	HR (95% CI)	P Value
Age, years (≥50/<50)	2.55 (1.74-3.73)	<0.001	2.10 (1.38-3.18)	<0.001
Sex (female/male)	0.84 (0.59-1.19)	0.318		
Body mass index (≥25/<25)	1.44 (0.98-2.08)	0.057		
HCV load (KIU/mL, ≥1,000/<1,000)	0.67 (0.43-1.03)	0.069		
Genotype (1/2)	0.73 (0.50-1.06)	0.098		
ALT (IU/L, ≥50/<50)	1.83 (1.14-2.94)	0.012		
Glucose level (prediabetes/normal)	2.25 (1.53-3.33)	<0.0001	2.19 (1.43-3.37)	<0.001
Triglyceride (mg/dL, ≥150/<150)	1.66 (0.93-2.98)	0.088		
Cholesterol (mg/dL, ≥220/<220)	1.56 (0.62-3.95)	0.346		
Histological diagnosis (LC/non-LC)	4.03 (2.55-6.36)	<0.0001	3.30 (2.06-5.28)	<0.001
Combination of ribavirin (−/+)	1.53 (0.99-2.38)	0.058		
Type of IFN (α/β)	0.88 (0.57-1.35)	0.882		
Total dose of IFN (MU, ≥500/<500)	0.91 (0.59-1.40)	0.672		
Efficacy (non-SVR/SVR)	2.73 (1.77-4.20)	<0.0001	2.78 (1.75-4.41)	<0.001

Data are expressed as the median (range).

Abbreviations: ALT, alanine aminotransferase; HR, hazard ratio; LC, liver cirrhosis.

prospectively followed. Another limitation of the study was that patients were treated with different types of antiviral therapy (IFN monotherapy or combination IFN + ribavirin therapy) for different duration (4 to 52 weeks). This heterogeneity makes it difficult to interpret the results of the study. On the other hand, the strength of the present study is the long-term follow-up in the large numbers of patients included.

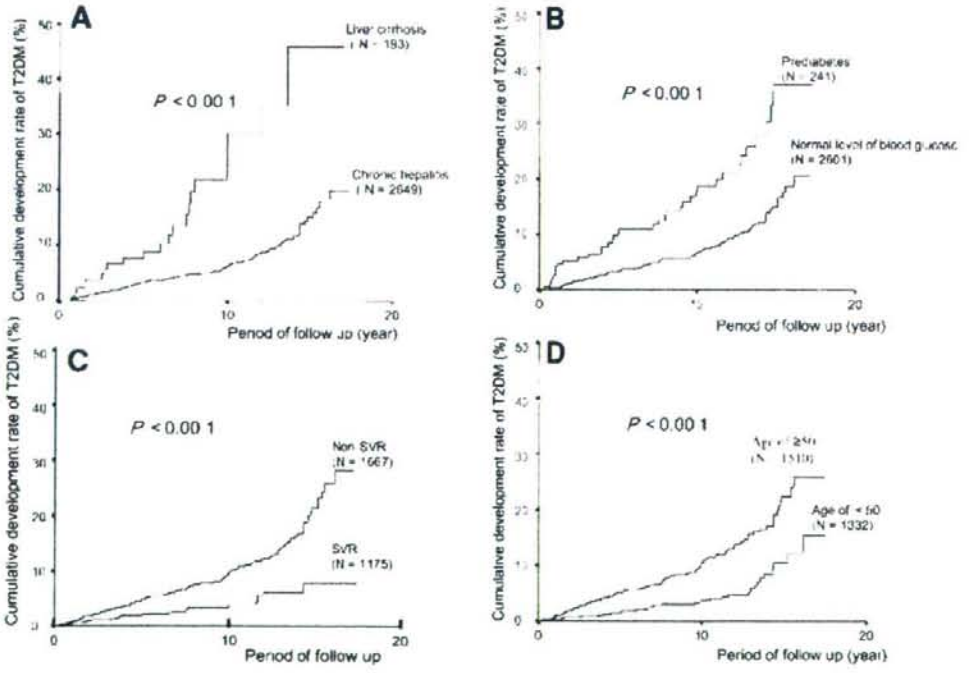

Fig. 2. Cumulative development rate of T2DM in patients treated with IFN. (A) Cumulative development rate of T2DM based on difference of hepatic fibrosis. (B) Cumulative development rate of T2DM based on the difference of glucose level. (C) Cumulative development rate of T2DM based on the difference of efficacy. (D) Cumulative development rate of T2DM based on the difference of age.

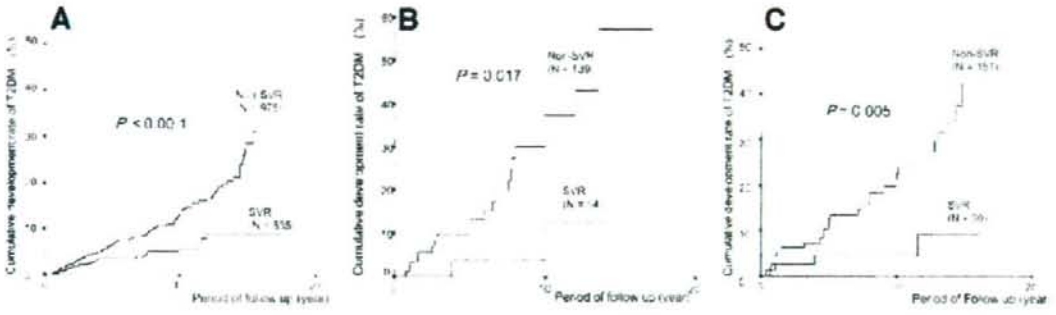

Fig. 3. Cumulative development rate of T2DM in patients with SVR or without SVR after IFN therapy. (A) Cumulative development rate of T2DM based on SVR or non-SVR in patients with age ≥50 years. (B) Cumulative development rate of T2DM based on SVR or non-SVR in patients with liver cirrhosis. (C) Cumulative development rate of T2DM based on the difference of SVR or non-SVR in patients with pre-diabetes.

The present study shows several findings with regard to development of T2DM after the termination of antivirus agents for HCV positive patients. First, the T2DM development rate in the non-SVR group was higher than that in the SVR group. The SVR caused a two-thirds reduction in the onset of T2DM in the course of posttreatment follow-up. That SVR reduced the onset of diabetes mellitus in HCV patients is in accordance with the data reported by Simó et al.[22] and Romero-Gómez et al.[23] Though the role of HCV in the pathogenesis of diabetes mellitus remains speculative, the following possible mechanisms have been reported: (1) patients with HCV have a tendency to attain insulin resistance[24]; (2) in transgenic mice, the expression of HCV core protein is associated with insulin resistance and T2DM development[25]; and (3) SVR in HCV patients reduces insulin resistance and onset of the incidence of abnormal glucose value.[26] Thus, it is accepted that clearance of HCV reduces the onset of T2DM.

Second, in addition to persistence of HCV, the present study suggests that aging, histological progression, and pre-diabetes enhanced the onset of T2DM in patients with HCV infection. However, when HCV was eradicated even in patients with age ≥50 years, pre-diabetes, or liver cirrhosis, the cumulative development rate of T2DM decreased.

T2DM is increasing dramatically in many Asian nations, including Japan, over the past decades.[27] It is widely accepted that 7 to 8 million people are affected by diabetes mellitus in Japan. Approximately 8% to 10% of adults in Japan have T2DM. In general, T2DM is associated with a genetic predisposition, but it is also strongly influenced by lifestyle-related factors, such as eating habits and/or physical activity.[28-33] The risk factors associated with T2DM include family history, age, sex, obesity, smoking, and physical activity. T2DM occurred in elderly patients compared to young patients. Life expectancies are long in Japan; thus, in the near future, a large number of patients with HCV will be >60 years of age. Therefore, it is apparent that the incidence of T2DM will increase in HCV-positive patients.

T2DM is a serious, costly disease. Treatment for T2DM may prevent some of its devastating complications, but does not usually restore normoglycemia or eliminate all the adverse consequences.[28,29] Moreover, HCV patients with T2DM are at major risk for HCC.[34] On the efficacy of IFN therapy, it has been reported that T2DM reduces HCV eradication via combination IFN + ribavirin therapy.[26] Thus, it should be considered whether HCV-positive patients should be treated with antiviral drugs in the histological nonprogression stage and at a non-elderly age for prevention of T2DM onset. If SVR obtained via antiviral therapy for HCV cannot only prevent progression to liver cirrhosis or HCC but also prevent the development of diabetes, the potential impact of IFN therapy is quite significant.

In conclusion, this retrospective study suggests that the annual incidence of T2DM among patients with HCV is 0.8% to 1.0%. Our results indicate that SVR causes a two-thirds reduction of T2DM development in HCV-positive patients treated with antiviral drugs.

Acknowledgment: The authors acknowledge the editorial assistance of Thomas Hughes.

References

1. Kiyosawa K, Furuta S. Review of hepatitis C in Japan. J Gastroenterol Hepatol 1991;6:383-391.
2. Alter MJ, Margolis HS, Krawczynski K, Judson FN, Mares A, Alexander WJ, et al. The natural history of community acquired hepatitis C in the United States. N Engl J Med 1992;327:1899-1905.
3. van Rossum TG, Vulto AG, de Man RA, Brouwer JT, Schalm SW. Review article: glycyrrhizin as a potential treatment for chronic hepatitis C. Aliment Pharmacol Ther 1998;12:199-205.

4. Colombo M, Kuo G, Choo QL, Donato MF, Del Ninno E, Tommasini MA, et al. Prevalence of antibodies to hepatitis C virus in Italian patients with hepatocellular carcinoma. Lancet 1989;2:1006-1008.
5. Hasan F, Jeffers LJ, De Medina M, Reddy KR, Parker T, Schiff ER, et al. Hepatitis C-associated hepatocellular carcinoma. HEPATOLOGY 1990;12: 589-591.
6. Kew MC, Houghton M, Choo QL, Kuo G. Hepatitis C virus antibodies in southern African blacks with hepatocellular carcinoma. Lancet 1990;335: 873-874.
7. Tsukuma H, Hiyama T, Tanaka S, Nakao M, Yabuuchi T, Kitamura T, et al. Risk factors for hepatocellular carcinoma among patients with chronic liver disease. N Engl J Med 1993;328:1797-1801.
8. Ikeda K, Saitoh S, Koida I, Arase Y, Tsubota A, Chayama K, et al. A multivariate analysis of risk factors for hepatocellular carcinogenesis: a prospective observation of 795 patients with viral and alcoholic cirrhosis. HEPATOLOGY 1993;18:47-53.
9. Gumber SC, Chopra S. Hepatitis C: a multifaceted disease- review of extrahepatic manifestations. Ann Intern Med 1995;123:615-620.
10. Johnson RJ, Gretch DR, Yamabe H, Hart J, Bacchi CE, Hartwell P, et al. Membranoproliferative glomerulonephritis associated with hepatitis C virus infection. N Engl J Med 1993;328:465-470.
11. Pawlotsky JM, Roudot-Thoraval F, Simmonds P, Mellor J, Ben Yahia MB, André C, et al. Extrahepatic immunologic manifestations in chronic hepatitis C and hepatitis C virus serotypes. Ann Intern Med 1995;122:169-173.
12. Boadas J, Rodriguez-Espinosa J, Enriquez J, Miralles F, Martínez-Cerezo FJ, González P, et al. Prevalence of thyroid autoantibodies is not increased in blood donors with hepatitis C virus infection. J Hepatol 1995;22:611-615.
13. Agnello V, Chung RT, Kaplan LM. A role for hepatitis C virus infection in type II cryoglobulinemia. N Engl J Med 1992;327:1490-1495.
14. Imazeki F, Yokosuka O, Fukai K, Kanda T, Kojima H, Saisho H. Prevalence of diabetes mellitus and insulin resistance in patients with chronic hepatitis C: comparison with hepatitis B virus-infected and hepatitis C virus-cleared patients. Liver Int 2008;28:355-362.
15. Arao M, Murase K, Kusakabe A, Yoshioka K, Fukuzawa Y, Ishikawa T, et al. Prevalence of diabetes mellitus in Japanese patients infected chronically with hepatitis C virus. J Gastroenterol 2003;38:355-360.
16. Genuth S, Alberti KG, Bennett P, Buse J, Defronzo R, Kahn R, et al. Expert Committee on the Diagnosis and Classification of Diabetes Mellitus. Follow-up report on the diagnosis of diabetes mellitus. Diabetes Care 2003;26:3160-3167.
17. Desmet VJ, Gerber M, Hoofnagle JH, Manns M, Sheuer PJ. Classification of chronic hepatitis: diagnosis, grading and staging. HEPATOLOGY 1994; 19:1513-1520.
18. Fleming TR, Harrington DP, O'Brien PC. Designs for group sequential tests. Control Clin Trials 1984;5:348-361.
19. Fabris P, Betterle C, Greggio NA, Zanchetta R, Bosi E, Biasin MR, et al. Insulin-dependent diabetes mellitus during alpha-interferon therapy for chronic viral hepatitis. J Hepatol 1998;28:514-517.
20. di Cesare E, Previti M, Russo F, Brancatelli S, Ingemi MC, Scoglio R, et al. Interferon-alpha therapy may induce insulin autoantibody development in patients with chronic viral hepatitis. Dig Dis Sci 1996;41:1672-1677.
21. Fajans S. Classification and diagnosis of diabetes. In: Rifkin H, Porte D, eds. Diabetes Mellitus: Theory and Practice. 4th ed. New York: Elsevier, 1990:346-356.
22. Simó R, Lecube A, Genescà J, Esteban JI, Hernández C. Sustained virological response correlates with reduction in the incidence of glucose abnormalities in patients with chronic hepatitis C virus infection. Diabetes Care 2006;29:2462-2466.
23. Romero-Gómez M, Fernández-Rodríguez CM, Andrade RJ, Diago M, Alonso S, Planas R, et al. Effect of sustained virological response to treatment on the incidence of abnormal glucose values in chronic hepatitis C. J Hepatol 2008;48:721-727.
24. Romero-Gómez M. Insulin resistance and hepatitis C. World J Gastroenterol 2006;12:7075-7080.
25. Shintani Y, Fujie H, Miyoshi H, Tsutsumi T, Tsukamoto K, Kimura S, et al. Hepatitis C virus infection and diabetes: direct involvement of the virus in the development of insulin resistance. Gastroenterology 2004;126:840-848.
26. Romero-Gómez M, Del Mar Viloria M, Andrade RJ, Salmerón J, Diago M, Fernández-Rodríguez CM, et al. Insulin resistance impairs sustained response rate to peginterferon plus ribavirin in chronic hepatitis C patients. Gastroenterology 2005;128:636-641.
27. Waki K, Noda M, Sasaki S, Matsumura Y, Takahashi Y, Isogawa A, et al. Alcohol consumption and other risk factors for self-reported diabetes among middle-aged Japanese: a population-based prospective study in the JPHC study cohort I. Diabet Med 2005;22:323-331.
28. Thuluvath PJ, John PR. Association between hepatitis C, diabetes mellitus, and race. a case-control study. Am J Gastroenterol 2003;98:438-441.
29. Mehta SH, Brancati FL, Strathdee SA, Pankow JS, Netski D, Coresh J, et al. Hepatitis C virus infection and incident type 2 diabetes. HEPATOLOGY 2003;38:50-56.
30. Wild S, Roglic G, Green A, Sicree R, King H. Global prevalence of diabetes: estimates for the year 2000 and projections for 2030. Diabetes Care 2004;27:1047-1053.
31. UK Prospective Diabetes Study (UKPDS) Group. Intensive blood-glucose control with sulphonylureas or insulin compared with conventional treatment and risk of complications in patients with type 2 diabetes (UKPDS 33). Lancet 1998; 352:837-853.
32. UK Prospective Diabetes Study (UKPDS) Group. Effect of intensive blood-glucose control with metformin on complications in overweight patients with type 2 diabetes (UKPDS 34). Lancet 1998;352: 854-865.
33. Elbein SC. The search for genes for type 2 diabetes in the post-genome era. Endocrinology 2002;143:2012-2018.
34. Veldt BJ, Chen W, Heathcote EJ, Wedemeyer H, Reichen J, Hofmann WP, et al. Increased risk of hepatocellular carcinoma among patients with hepatitis C cirrhosis and diabetes mellitus. HEPATOLOGY 2008;47:1856-1862.

RESEARCH ARTICLES

ERK5 is a Target for Gene Amplification at 17p11 and Promotes Cell Growth in Hepatocellular Carcinoma by Regulating Mitotic Entry

Keika Zen,[1] Kohichiroh Yasui,[1]* Tomoaki Nakajima,[1] Yoh Zen,[2] Kan Zen,[3] Yasuyuki Gen,[1] Hironori Mitsuyoshi,[1] Masahito Minami,[1] Shoji Mitsufuji,[1] Shinji Tanaka,[4] Yoshito Itoh,[1] Yasuni Nakanuma,[2] Masafumi Taniwaki,[5] Shigeki Arii,[4] Takeshi Okanoue,[1] and Toshikazu Yoshikawa[1]

[1]Molecular Gastroenterology and Hepatology, Graduate School of Medical Science, Kyoto Prefectural University of Medicine, Kyoto, Japan
[2]Department of Human Pathology, Kanazawa University Graduate School of Medicine, Kanazawa, Japan
[3]Division of Cardiovascular Medicine, Omihachiman Community Medical Center, Omihachiman, Japan
[4]Department of Hepato-Biliary-Pancreatic Surgery, Tokyo Medical and Dental University, Tokyo, Japan
[5]Molecular Hematology and Oncology, Graduate School of Medical Science, Kyoto Prefectural University of Medicine, Kyoto, Japan

Using high-density oligonucleotide microarrays, we investigated DNA copy-number aberrations in cell lines derived from hepatocellular carcinomas (HCCs) and detected a novel amplification at 17p11. To identify the target of amplification at 17p11, we defined the extent of the amplicon and examined HCC cell lines for expression of all seven genes in the 750-kb commonly amplified region. Mitogen-activated protein kinase (MAPK) 7, which encodes extracellular-regulated protein kinase (ERK) 5, was overexpressed in cell lines in which the gene was amplified. An increase in *MAPK7* copy number was detected in 35 of 66 primary HCC tumors. Downregulation of *MAPK7* by small interfering RNA suppressed the growth of SNU449 cells, the HCC cell line with the greatest amplification and overexpression of *MAPK7*. ERK5, phosphorylated during the G2/M phases of the cell cycle, regulated entry into mitosis in SNU449 cells. In conclusion, our results suggest that *MAPK7* is likely the target of 17p11 amplification and that the ERK5 protein product of *MAPK7* promotes the growth of HCC cells by regulating mitotic entry.

INTRODUCTION

Hepatocellular carcinoma (HCC) is the fifth most common malignancy in the world and is estimated to cause approximately half a million deaths annually (El-Serag, 2002). Several risk factors for HCC have been reported, including infection with hepatitis B and C viruses, dietary intake of afratoxin, alcohol consumption, and diabetes.

The mitogen-activated protein kinase (MAPK) cascades transmit extracellular signals from cell surface receptors to specific intracellular targets and regulate a wide variety of cellular functions, including cell proliferation, differentiation, and the stress response (Nishimoto and Nishida, 2006). Extracellular stimuli induce sequential activation of MAPK kinase kinase, MAPK kinase, and MAPK. At least four MAPK subfamilies have been identified: extracellular-regulated protein kinase (ERK) 1 and 2, c-Jun-N-terminal kinases, p38, and ERK5 (also know as BMK1). ERK5, which was recently characterized, can be activated by a wide range of growth factors and cellular stresses, including serum, epithelial growth factor, oxidative stress, and hyperosmotic shock (Hayashi and Lee, 2004; Nishimoto and Nishida, 2006; Wang and Tournier, 2006). When stimulated, MAP/ERK kinase kinase 2 and 3 activate MAP/ERK kinase (MEK) 5, a specific kinase for ERK5. Subsequently, MEK5 phosphorylates ERK5, and the activated ERK5 promotes cell proliferation, differentiation, and survival (Hayashi and Lee, 2004; Garaude et al., 2006; Nishimoto and Nishida, 2006; Wang and Tournier, 2006). Some investigators have described the possible involvement of ERK5 in cancers (Esparis-Ogando et al., 2002; Weldon et al., 2002; Mulloy et al., 2003; Carvajal-Vergara et al., 2005; Linnerth et al., 2005).

Additional Supporting Information may be found in the online version of this article.

Supported by: Grants-in-Aid for Scientific Research from the Japan Society for the Program of Science, Grant number: 18390223.

*Correspondence to: Kohichiroh Yasui, Molecular Gastroenterology and Hepatology, Graduate School of Medical Science, Kyoto Prefectural University of Medicine, 465 Kajii-cho, Kamigyo-ku, Kyoto, 602-8566, Japan. E-mail: yasuik@koto.kpu-m.ac.jp

Received 24 May 2008; Accepted 11 September 2008
DOI 10.1002/gcc.20624
Published online 30 October 2008 in Wiley InterScience (www.interscience.wiley.com).

Accumulating evidence suggests that multiple sequential genetic alterations in a cell lineage at the nucleotide and chromosome levels underlie the carcinogenesis of solid tumors. Amplification of chromosomal DNA is one mechanism of activating genes whose overexpression contributes to the development and progression of cancer. Regions of chromosomal amplification in cancer cells frequently harbor oncogenes, such as *MYC* (Little et al., 1983) and *ERBB2* (Di Fiore et al., 1987). Using comparative genomic hybridization (CGH), we have detected novel regions of amplification in a variety of cancer types, including HCC, and we have identified a number of candidate oncogenes from amplicons (Yasui et al., 2001; Yasui et al., 2002; Yokoi et al., 2002; Okamoto et al., 2003; Yokoi et al., 2003). CGH was initially used for genome-wide detection of copy number changes occurring in cancers (Kallioniemi et al., 1992). However, its resolution is limited (5–10 Mb) because it detects segmental copy number changes on metaphase chromosomes.

The recent introduction of high-density oligonucleotide microarrays designed for typing of single nucleotide polymorphisms (SNPs) facilitates high-resolution mapping of chromosomal amplifications, deletions, and loss of heterozygosity (Mei et al., 2000; Bignell et al., 2004; Matsuzaki et al., 2004a,b; Wong et al., 2004; Zhao et al., 2004). The Affymetrix GeneChip Mapping 100K array set contains 116,204 SNP loci with a mean intermarker distance of 23.6 kb, and it enables detailed and genome-wide identification of DNA copy number changes (Matsuzaki et al., 2004a,b; Garraway et al., 2005; Zhao et al., 2005). The newer GeneChip Mapping 500K array set is composed of two arrays, each capable of genotyping an average 250,000 SNPs.

In the work reported here, we investigated DNA copy number aberrations in HCC cell lines using Affymetrix high-density SNP arrays. We identified a novel amplification at 17p11 in HCC cell lines. This region may harbor one or more genes that, when amplified, contribute to carcinogenesis. Within the amplicon, *MAPK7*, which encodes ERK5, emerged as a probable target gene that acts as a driving force for amplification of the region and promotes the growth of HCC cells by regulating entry into mitosis.

MATERIALS AND METHODS

Cell Lines and Tumor Samples

A total of 21 liver cancer cell lines [HCC-derived HLE, HLF (Dor et al., 1975), PLC/PRF/5 (Alexander et al., 1976), Li7 (Hirohashi et al., 1979), Huh7 (Nakabayashi et al., 1982), Hep3B (Aden et al., 1979), SNU354, SNU368, SNU387, SNU398, SNU423, SNU449, SNU475 (Park et al., 1995), JHH-1, JHH-2, JHH-4, JHH-5, JHH-6, JHH-7 (Fujise et al., 1990), Huh-1 (Huh et al., 1981), and the hepatoblastoma line HepG2 (Knowles et al., 1980)] were examined in this study. All cell lines were maintained in Dulbecco's modified Eagle's medium supplemented with 10% fetal bovine serum. We obtained 66 primary HCC tumors for analysis of the DNA copy number of *MAPK7* from patients undergoing surgery at the hospitals of Tokyo Medical and Dental University and Kyoto University, Japan. Genomic DNA was isolated from each cell line and from 66 primary tumors using the Puregene DNA isolation kit (Gentra, Minneapolis, MN). For immunohistochemical studies of ERK5, 43 additional HCC samples were obtained from the Hospital of Kyoto Prefectural University of Medicine, Japan. Before initiation of the present study, informed consent was obtained in the formal style approved by all relevant ethical committees.

SNP Assay

The GeneChip Mapping 100K array set and GeneChip Mapping 250K Sty array (Affymetrix, Santa Clara, CA) were used in this study. Analyses were performed according to the manufacturer's instructions. In brief, 250 ng of genomic DNA was digested with a restriction enzyme (*Xba*I or *Hind*III for the 100K array set and *Sty*I for the 250K Sty array), ligated to an adaptor, and amplified by PCR (Kennedy et al., 2003; Matsuzaki et al., 2004a,b; Zhao et al., 2004). Amplified products were fragmented, labeled by biotinylation, and hybridized to the microarrays. Hybridization was detected by incubation with a streptavidin-phycoerythrin conjugate, followed by scanning of the array, and analysis was performed as described previously (Kennedy et al., 2003; Di et al., 2005). Copy number changes were calculated using the Copy Number Analyzer for Affymetrix GeneChip Mapping Arrays (http://www.genome.umin.jp) (Nannya et al., 2005).

Fluorescence In Situ Hybridization

We performed FISH using the bacterial artificial chromosome (BAC) RP11-73E4 as a probe (Invitrogen, Carlsbad, CA) as described previously (Yasui et al., 2002). The BAC was selected

on the basis of its location according to the database provided by the UCSC (http://genome.ucsc.edu/). Briefly, the probe was labeled by nick translation with biotin-16-dUTP (Roche Diagnostics, Penzberg, Germany) and hybridized to metaphase chromosomes. Hybridization signals for biotin-labeled probes were detected with avidin-fluorescein (Roche Diagnostics).

Real-Time Quantitative PCR

We quantified genomic DNA and mRNA using a real-time fluorescence detection method. Total RNA was obtained using Trizol (Invitrogen). Residual genomic DNA was removed by incubating the RNA samples with RNase-free DNase I (Takara Bio, Shiga, Japan) prior to reverse transcription (RT)-PCR. Single-stranded complementary DNA was generated using superscript III reverse transcriptase (Invitrogen) according to the manufacturer's directions. Real-time quantitative PCR experiments were performed with the LightCycler system using FastStart DNA Master Plus SYBR Green I (Roche Diagnostics) according to the manufacturer's protocol. The primers were as follows: *MAPK7* DNA (forward, 5′-TGCTGACTGGCTCGAAG-3′; reverse, 5′-GGGTCTGAGATGAACCTGC-3′); *MAPK7* mRNA (forward, 5′-TTTGCCTTACTTCCCACCTG-3′; reverse, 5′-CCCATGTCGAAAGACTGGTT-3′); *GRAP* mRNA (forward, 5′-TCGAAGGACAGACTGCACAC-3′; reverse, 5′-AGAAGAGGAGTGTGCCTCCA-3′); *EPN2* mRNA (forward, 5′-TCACCTCACCCACCACTGTA-3′; reverse, 5′-GTGGTCAGCTGCCCTTAGAG-3′); *EPPB9* mRNA (forward, 5′-CTTTGTGTACGGCCAGGACT-3′; reverse, 5′-CGTAGGGGTTGGTGCTTTTA-3′); *MFAP4* mRNA (forward, 5′-GGTGACTCCCTGTCCTACCA-3′; reverse, 5′-TCATCTCAGTGCGTTTGAGG-3′); *ZNF179* mRNA (forward, 5′-ACTGGGCAGAACCAGAGAGA-3′; reverse, 5′-AGGATGCACAGACAGGCTCT-3′); *FLJ10847* mRNA (forward, 5′-AACTCTTGGGCTTCAAGCAA-3′; reverse, 5′-AGGAGGTTGAGGCTGCAGTA -3′). These primers were designed using Primer3 (http://frodo.wi.mit.edu/cgi-bin/primer3/primer3_www.cgi) on the basis of sequence data obtained from the NCBI database (http://www.ncbi.nlm.nih.gov/). *GAPDH* (Minamiya et al., 2004) and long interspersed nuclear element (LINE)-1 (Zhao et al., 2004) were used as endogenous controls for mRNA and genomic DNA levels, respectively.

Immunoblotting

Immunoblots were prepared according to previously reported methods (Yasui et al., 2001). Cell lysates (20 μg protein per sample) were separated by sodium dodecyl sulfate-polyacrylamide gel electrophoresis on 10% acrylamide gels. We obtained the following antibodies from Sigma-Aldrich (Tokyo, Japan): anti-ERK5 polyclonal antibody, anti-phospho-ERK5 (pThr218/pThr220) polyclonal antibody, and anti-β-actin monoclonal antibody. For immunoblotting, we used anti-ERK5, anti-phospho-ERK5, and anti-β-actin at dilutions of 1:500, 1:1000, and 1:5000, respectively. For secondary immunodetection, we used anti-rabbit or anti-mouse Ig (Amersham, Tokyo, Japan) diluted 1:5000. Protein binding was detected using the ECL system (Amersham).

Immunoprecipitation

Cells were lysed with RIPA buffer (10 mM Tris-HCl, pH 7.4, 150 mM NaCl, 1% Triton X-100, 0.1% sodium dodecyl sulfate, 1% sodium deoxycholate, 1 mM phenylmethylsulfonyl fluoride), and incubated on ice for 30 min. The lysate was centrifuged at 14,000 × *g* at 4°C for 15 min. The supernatant was incubated with normal rabbit IgG and protein A-agarose beads (Santa Cruz Biotechnology, Santa Cruz, CA) to decrease nonspecific protein binding. After centrifugation, the supernatant was incubated with anti-ERK5 polyclonal antibody or normal rabbit IgG (control) overnight at 4°C. Protein A-agarose beads were added to the reaction and the mixture was incubated for an additional 1 hr. The precipitates were recovered by a brief centrifugation, followed by four washes with RIPA buffer. Samples were then boiled in electrophoresis sample buffer and separated by electrophoresis as described above (see "Immunoblotting" section).

Immunohistochemical Analysis

Forty-three primary HCCs, consisting of paired tumor and surrounding nontumor tissues, and two HCC cell lines (SNU449 and Li7) were analyzed by anti-ERK5 immunostaining. Immunohistochemical staining was performed on formalin-fixed and paraffin-embedded sections using an anti-ERK5 polyclonal antibody (Sigma-Aldrich) at a 1:200 dilution. An automated tissue immunostainer (Ventana Medical Systems, Tucson, AZ) was used according to the manufacturer's instructions. The staining was developed with 3,3′-

diaminobenzidine tetrahydrochloride, followed by counterstaining with hematoxylin.

Growth Assays and RNA Interference Studies

For cell growth assays viable cells were stained with 0.2% trypan blue and counted with a hemocytometer 24, 48, and 72 hr after transfection. For RNA interference (RNAi) studies, Stealth small interfering RNA (siRNA) duplex oligoribonucleotides targeting *MAPK7* (5′-CCAUGGCAUGAACCCUGCCGAUAUU-3′) and Stealth RNAi negative control duplexes were synthesized by Invitrogen. The siRNAs were delivered into SNU449 cells using Lipofectamine 2000 (Invitrogen) according to the manufacturer's instructions. To determine mRNA levels, cells were harvested 48 hr after transfection and subjected to quantitative RT-PCR as described above.

Cell Cycle Synchronization

SNU449 cells were synchronized at G1/S, early S, or M phases. For G1/S or early S-phase synchronization, cells were incubated in medium containing 2.5 mM thymidine (Sigma Chemical Co., St. Louis, MO) for 24 hr, followed by 12 hr in medium without thymidine, and finally another 12 hr in medium containing 2.5 mM thymidine (double-thymidine block; for G1/S-phase) or 1 μg/ml aphidicolin (early S-phase block). For M phase synchronization, cells were incubated in medium containing 2.5 mM thymidine for 24 hr, followed by 4 hr in medium without thymidine, and finally another 12 hr in medium containing 0.5 μg/ml nocodazole.

Cell Cycle Analysis

SNU449 cells were synchronized at the G1/S-phase boundary by a double-thymidine block as described above. Synchronized cells were released into fresh medium without thymidine and harvested at the indicated time points. These cells were then stained with propidium iodide and analyzed using a FACSCaliber scanner and Cell Quest software (Becton Dickinson Pharmingen, San Diego, CA).

Mitotic Index

Cells were grown in 24-well plates and transfected with Stealth RNAi targeting *MAPK7* or Stealth RNAi negative control duplexes as described above (see "Growth Assays and RNA Interference Studies" section). After 24 hr, cells were synchronized at the G1/S-phase boundary by a double-thymidine block. Synchronized cells were collected, reseeded on glass slides, and incubated for an additional 9 hr in fresh medium without thymidine. Next, the cells were stained with an anti-phospho-histone H3 antibody that specifically detects mitotic cells. Briefly, cells were fixed with 3.7% formaldehyde, permeabilized with 0.25% Triton X-100, and incubated with PBS containing 1% bovine serum albumin. The cells were then treated with a mixture of 4 μg/ml anti-phospho-histone H3 (Ser10)-biotin conjugated antibody (Upstate Biotechnology, Lake Placid, NY) and a 1:100 dilution of streptavidin-fluorescein (Roche Diagnostics) for 1 hr at room temperature, followed by counterstaining with propidium iodide. Positive staining for phospho-histone H3 was quantified by counting stained cells under a fluorescence microscope and dividing by the number of total cells. The mitotic index was scored as the percentage of mitotic cells in a population. On average, 200 cells were scored in three separate areas.

Statistical Analysis

All statistical analyses were performed using SPSS 15.0 software (SPSS Inc., Chicago, IL). Chi-square tests or analysis of variance (ANOVA) were used. P values < 0.05 were considered significant.

RESULTS

Detection of the 17p11 Amplicon in HCC Cell Lines by SNP Array Analysis

We screened for DNA copy number aberrations in 20 HCC cell lines by SNP array analysis. Two of the 20 cell lines, SNU449 and JHH-7, exhibited amplifications at chromosomal band 17p11 (Fig. 1A). In particular, the SNU449 cell line showed a high level of amplification in a narrow region on 17p11. We were able to define the smallest commonly affected region in the 17p11 amplicon as that lying between the positions recognized by the Affymetrix SNP_A-1662618 and SNP_A-1720748 probes (Fig. 1B). This region includes seven known or predicted protein-coding genes, *GRAP*, *EPN2*, *EPPB9*, *MAPK7*, *MFAP4*, *ZNF179*, and *FLJ10847*. The size of the amplicon was estimated to be approximately 750 kb.

To confirm amplification at 17p11 in SNU449 cells, we performed FISH analysis. The probe for

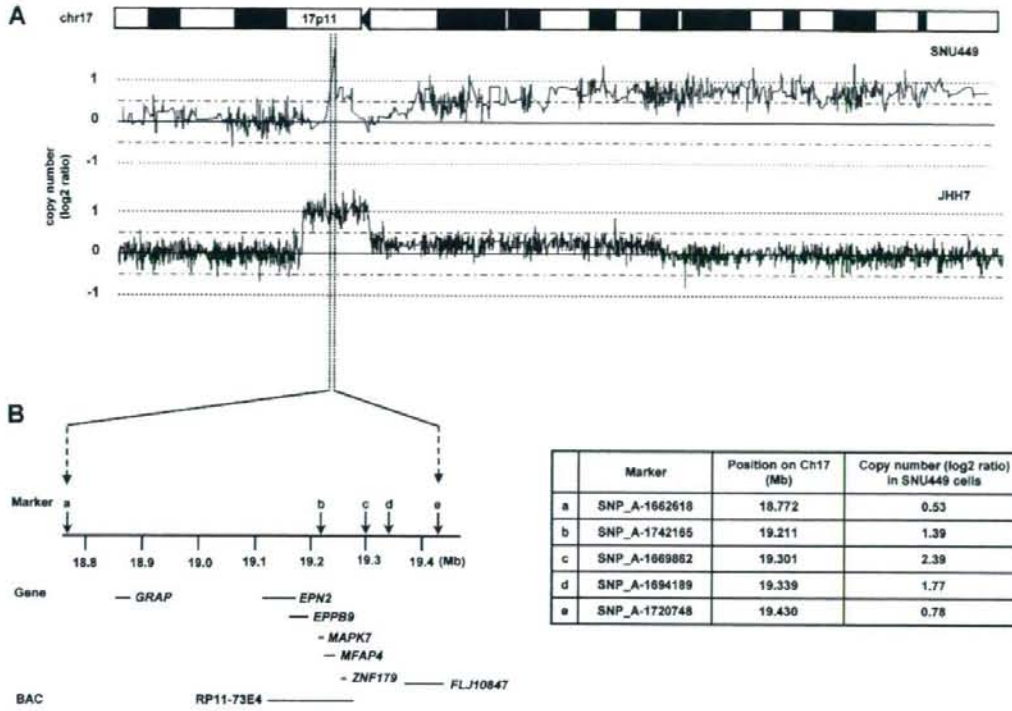

	Marker	Position on Ch17 (Mb)	Copy number (log2 ratio) in SNU449 cells
a	SNP_A-1662618	18.772	0.53
b	SNP_A-1742165	19.211	1.39
c	SNP_A-1669862	19.301	2.39
d	SNP_A-1694189	19.339	1.77
e	SNP_A-1720748	19.430	0.78

Figure 1. Map of the amplicon at 17p11 in two HCC cell lines. A: Copy number profiles for chromosome 17 in SNU449 and JHH-7 cells. Copy number values were determined by SNP 100K and 250K array analyses for SNU449 and JHH-7 cells, respectively. B: The smallest common region of amplification in SNU449 and JHH-7 cells (left). The position of the Affymetrix SNP markers, the seven genes within the amplicon (*GRAP, EPN2, EPPB9, MAPK7, MFAP4, ZNF179*, and *FLJ10847*) and the BAC RP11-73E4 (used as a probe for FISH) are numbered according to the UCSC genome database (http://genome.ucsc.edu/). Detailed copy-number information at positions identified by individual SNP markers over the amplified region in SNU449 cells is shown at right.

these experiments was BAC RP11-73E4, which contains *EPN2*, *EPPB9*, *MAPK7*, *MFAP4*, and *ZNF179* (Fig. 1B). This probe showed an amplified FISH signal on metaphase chromosomes from SNU449 cells (Fig. 2A). To further characterize the relationship between the genes in this chromosomal region and amplifications observed in cancer cells, we analyzed the gene dosage of the *MAPK7* locus by real-time quantitative PCR of DNA from 21 different liver cancer cell lines (20 HCC cell lines and the hepatoblastoma line HepG2). Amplification of *MAPK7* was observed in SNU449 and JHH-7 cells (Fig. 2B). Taken together, the data provide strong evidence that the 17p11 region is amplified in SNU449 and JHH-7 cells.

Analysis of Positional Candidate Genes in HCC Cell Lines

The 17p11 region may harbor one or more genes (henceforth referred to as "target genes") that, when activated by amplification, play a role in carcinogenesis. A common criterion for designating a gene as a putative target is that amplification leads to its overexpression (Collins et al., 1998). Thus, using real-time quantitative PCR, we determined the mRNA levels of all seven genes in the 17p11 amplicon in our panel of 21 liver cancer cell lines. As shown in Fig. 2C, the *EPN2*, *EPPB9*, and *MAPK7* genes were overexpressed in both SNU449 and JHH-7 cells. In several other lines, one or more of these three genes was overexpressed, despite the fact that regional amplification was not observed. These findings suggest that *EPN2*, *EPPB9*, and *MAPK7* are candidate target genes for 17p11 amplification.

Of these three genes, we chose to focus further analysis on *MAPK7*, which encodes ERK5, because ERK5-related proteins have been previously implicated in carcinogenesis (Hayashi and Lee, 2004; Wang and Tournier, 2006), whereas there is little or no evidence linking *EPN2* or

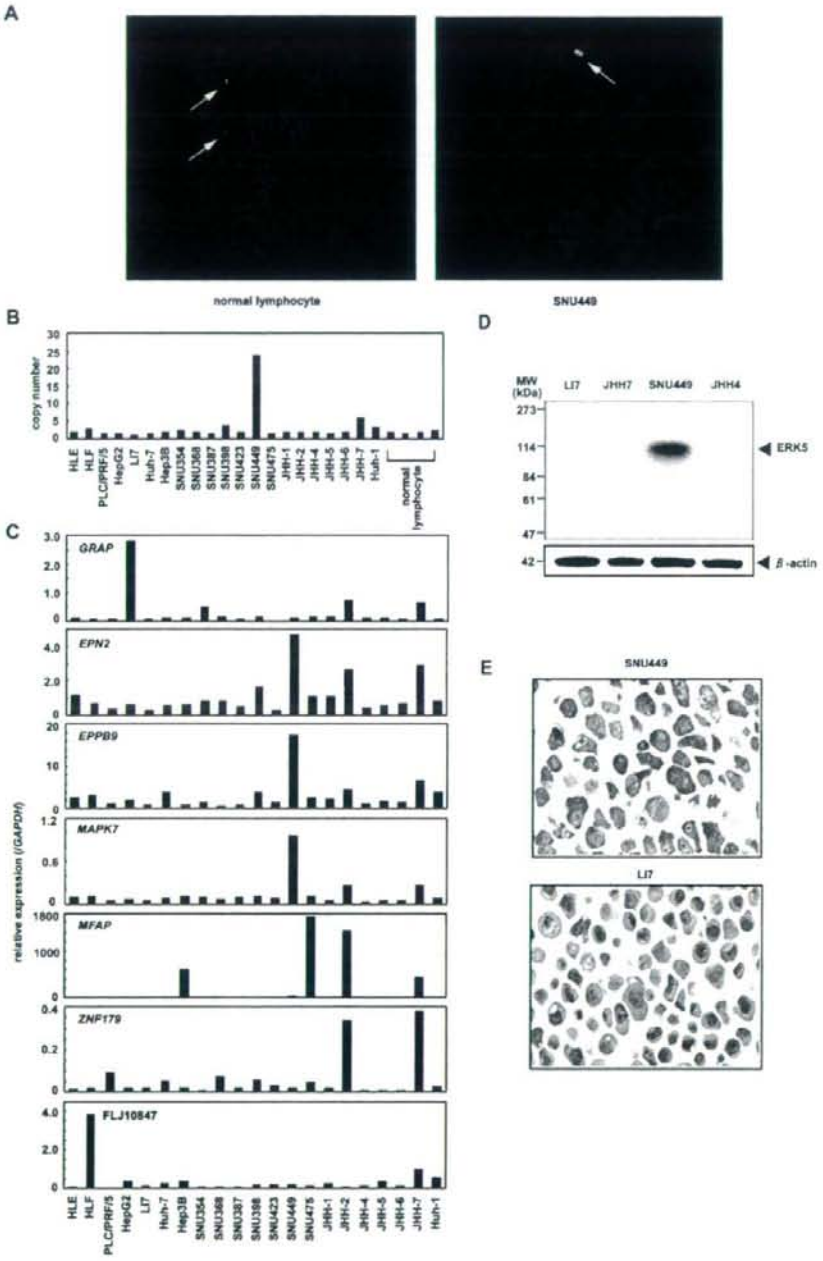

Figure 2. Amplification and overexpression of *MAPK7* in HCC cell lines. (A) Representative images from FISH analysis using a BAC RP11-73E4 probe on metaphase chromosomes from normal lymphocytes and SNU449 cells. While the probe shows a normal signal pattern (2 copies/cell) in normal lymphocytes (arrows, left), it shows an amplified signal in SNU449 cells (arrow, right). (B) Copy number of *MAPK7* in 21 liver cancer cell lines (20 HCC cells and one hepatoblastoma line, HepG2) and four peripheral blood lymphocytes (normal cell controls) as measured by real-time quantitative PCR with reference to a LINE-1 control. Values were normalized such that the average copy number of *MAPK7* in genomic DNA derived from normal lymphocytes is 2. (C) Relative expression levels of the seven genes within the 17p11 amplicon in a panel of 21 liver cancer cell lines as determined by real-time quantitative RT-PCR. The results are presented as the ratio between the expression level of each gene and a reference gene (*GAPDH*) to correct for variation in the amount of RNA. (D) Immunoblot analysis to detect protein levels of ERK5 and β-actin, an internal control, in four HCC cell lines with different *MAPK7* DNA copy numbers (B) and mRNA levels (C). (E) Immunostaining of ERK5 in SNU449 and Li7 cells.

EPPB9 to tumorigenesis. Immunoblot analysis revealed that ERK5 expression is upregulated in SNU449 cells. Indeed, among the HCC cell lines that were tested, SNU449 showed the highest level of both 17p11 amplification and *MAPK7* overexpression (Fig. 2D). Moreover, immunostaining confirmed that the level of ERK5 was elevated in SNU449 cells. ERK5 was strongly expressed in the cytoplasm of SNU449 cells (Fig. 2E). In contrast, ERK5 was weakly expressed in only a few Li7 cells, a HCC cell line that shows neither amplification nor overexpression of *MAPK7* (Fig. 2E).

Copy Number Gain of *MAPK7* in Primary HCC Tumors

To determine whether *MAPK7* is amplified in primary tumors, we examined 66 primary HCCs for copy number gains using real-time quantitative PCR. Copy number changes were counted as gains if the results of the analysis for a given tumor cell type exceeded the mean plus twice the standard deviation (SD) of the levels of *MAPK7* observed in genomic DNA derived from four peripheral blood lymphocyte samples (i.e., normal cells). A copy number gain for *MAPK7* was observed in 35 of the 66 tumors (53%; Fig. 3).

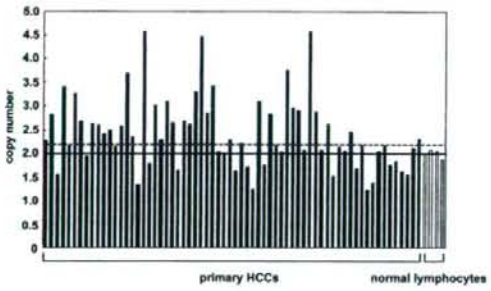

Figure 3. Copy number gain of *MAPK7* in primary HCC tumors. Copy numbers of *MAPK7* in 66 primary HCC tumors and four normal peripheral blood lymphocytes were determined by real-time quantitative PCR with reference to a LINE-1 control. Values were normalized such that the average copy number of *MAPK7* in genomic DNA derived from the normal lymphocytes equals 2 (solid horizontal line). The mean + 2 × SD of normal lymphocytes was used as the cutoff value for copy number gain (dotted line).

Expression of ERK5 in Primary HCCs

We next examined the level of ERK5 in 43 additional primary HCCs, including paired tumor and surrounding nontumor tissues. Immunohistochemical studies revealed that, in nontumor tissues (normal liver, chronic hepatitis, or liver cirrhosis), ERK5 is strongly expressed in bile ducts, bile ductules, and a few small hepatocytes (Fig. 4A). In these cells, ERK5 was present in the cytoplasm. Hepatocytes also contained ERK5, although at a lower level than in bile ducts (Fig. 4A). The staining pattern for ERK5 was almost identical for normal liver, chronic hepatitis, and liver cirrhosis.

This granular cytoplasmic staining for ERK5 was also observed in HCC cancer cells (Fig. 4B). HCC cells containing ERK5 were uniformly distributed in the tumor tissues. The level of ERK5 was elevated in 11 of the 43 tumors compared with the paired nontumor tissues (Figs. 4B and 4C; Supp. Info. Table 1). To clarify the relationship between the level of ERK5 and various clinicopathological parameters, we examined available data from the 43 patients, whose tumors were divided into elevated (T>NT) and not elevated (T≤NT) groups. There was no significant correlation between the level of ERK5 and any parameter examined, including age and gender of the patients; size, stage, and degree of differentiation of the tumor; HBV or HCV infection; and

Figure 4. Representative ERK5 immunostaining of tissues. (A) A nontumorous liver tissue (chronic hepatitis). The level of ERK5 is elevated in the bile duct (large arrow), bile ductules (arrowheads), and a few small hepatocytes (small arrow). (B, C) Paired tumor (B) and nontumor (C) tissues from one HCC patient, wherein the level of ERK5 is elevated in the tumor compared with the counterpart nontumor tissue. Original magnification, ×400.

features of nontumorous liver tissues (Supp. Info. Table 1).

Downregulation of *MAPK7* Inhibits the Growth of HCC Cells

To investigate the effects of *MAPK7* overexpression on HCC cells, we knocked down its expression using RNAi. In SNU449 cells treated with siRNA targeting *MAPK7*, we observed a decrease in *MAPK7* mRNA and ERK5 protein levels relative to that observed for cells receiving a control siRNA or transfection agent alone (Figs. 5A and 5B). The siRNA-mediated downregulation of *MAPK7* suppressed the growth of SNU449 cells at all time points assayed over a 72-hr period (Fig. 5C). These findings suggest that ERK5 promotes the growth of HCC cells.

ERK5 is Phosphorylated During the G2/M Phases of the Cell Cycle

To help elucidate the underlying mechanism by which ERK5 regulates cellular proliferation we investigated the role of ERK5 in cell cycle progression. SNU449 cells were synchronized at G1/S, early S, or M phases of the cell cycle using a double-thymidine, aphidicolin, or nocodazole block, respectively. We determined the levels of total ERK5 and phosphorylated (active) form of ERK5. Immunoblotting did not show a difference in the level of total ERK5 among the three phases of the cell cycle (Fig. 6A). To detect phosphorylated ERK5, total ERK5 was immunoprecipitated from cell lysates using an anti-ERK5 antibody and then analyzed by immunoblotting using an anti-phospho-ERK5 antibody. Phosphorylated ERK5 was more abundant in cells synchronized at the M phase than in asynchronous cells (Fig. 6B).

We next synchronized SNU449 cells at the G1/S boundary using a double-thymidine block and then released the cells from the block. Using flow cytometry, we confirmed the synchrony of the cell cycle and monitored its progression after removal of thymidine (Fig. 6C). There was no difference in the level of total ERK5 during progression of the cell cycle (Fig. 6D). Expression of phosphorylated ERK was maximal 9 hr after release from the block (Fig. 6E), a time when a large proportion of cells were in the G2/M phase (Fig. 6C). Taken together, these observations indicate that ERK5 is phosphorylated during the G2/M phases of the cell cycle.

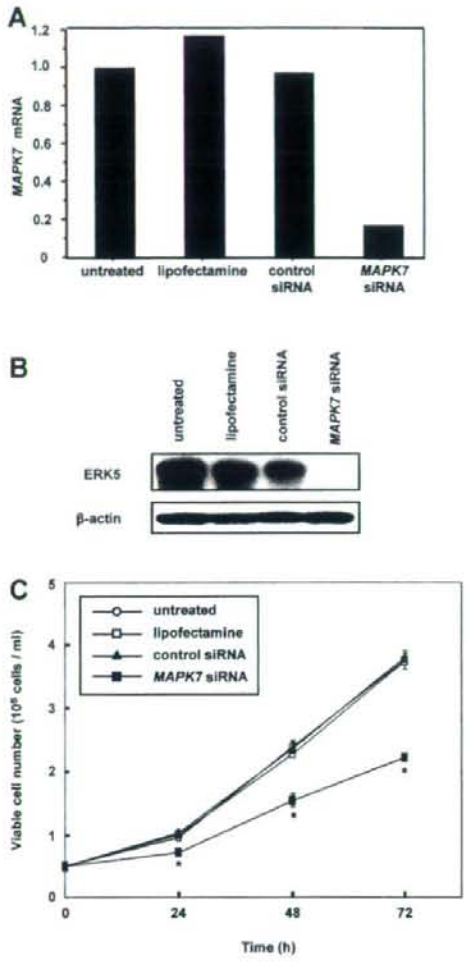

Figure 5. Growth inhibition of SNU449 cells by knockdown of *MAPK7*. A: Relative expression levels of *MAPK7* mRNA as determined by real-time quantitative RT-PCR. SNU449 cells were treated with siRNA targeting *MAPK7*, negative control siRNA, or the transfection agent alone (Lipofectamine), and harvested 48 hr after transfection. Untreated cells were maintained under identical experimental conditions. Results are presented as a ratio between the expression level of *MAPK7* and that of a reference gene (*GAPDH*) to correct for variation in the amount of RNA. Relative expression levels were normalized such that the ratio in untreated cells is 1. B: Levels of ERK5 and β-actin, an internal control, determined by immunoblotting. C: Cell growth was assayed by counting the viable cells at the indicated times after transfection. Each assay was performed in triplicate. Values are represented as the mean ± SD. Differences were analyzed by ANOVA (*$P < 0.01$).

ERK5 Regulates Entry into Mitosis

Our results indicating that ERK5 is activated during the G2/M phases in SNU449 cells suggested that ERK5 may be involved in G2/M progression. To examine whether ERK5 plays a role in mitotic entry, we knocked down *MAPK7*

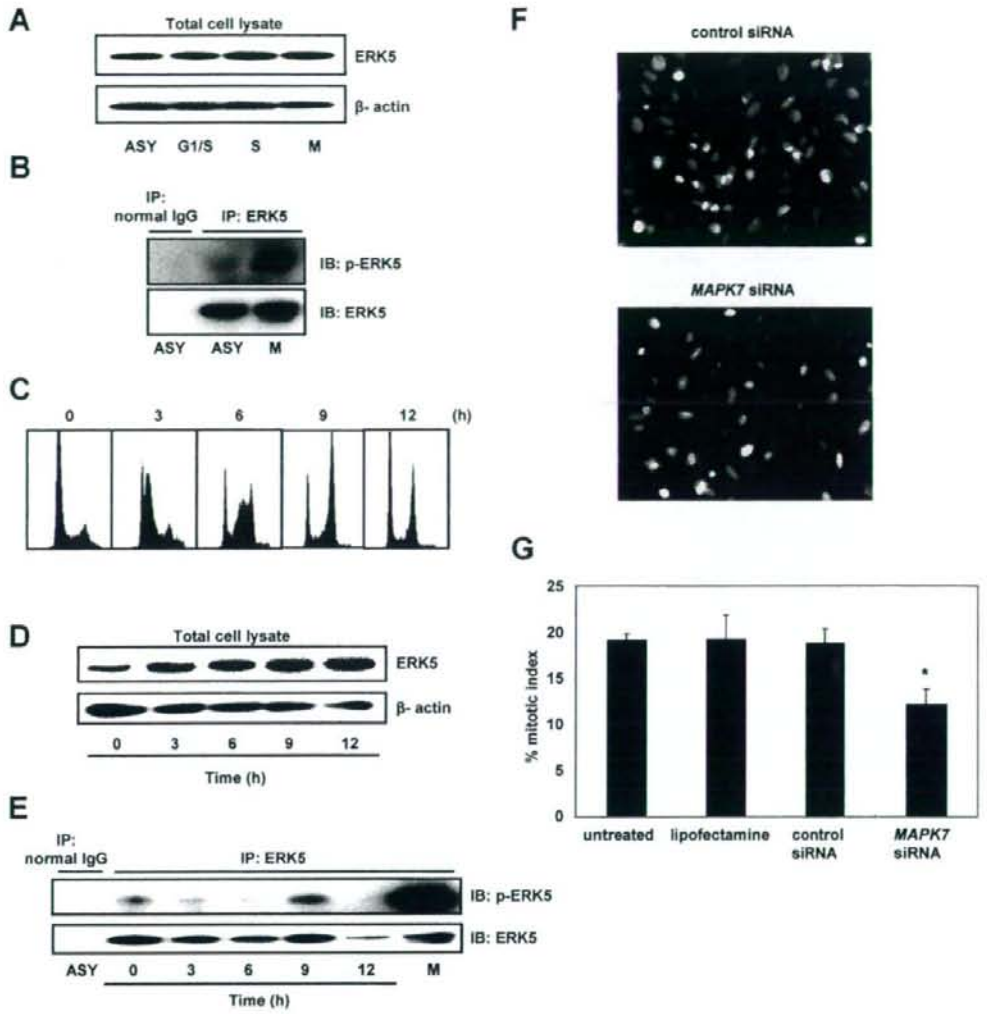

Figure 6. ERK5 is phosphorylated during the G2/M phases of the cell cycle. (A) Immunoblot analysis to detect protein levels of total ERK5 and β-actin, an internal control, in SNU449 cells that were synchronized at the G1/S, early S, or M phases using a double-thymidine, aphidicolin, or nocodazole block, respectively, or were untreated and used as an asynchronous (ASY) population. (B) Levels of phosphorylated ERK5 (p-ERK5). ERK5 was immunoprecipitated (IP) from lysates of SNU449 cells that were synchronized at the M phase (M) or from asynchronous cells (ASY). The samples were split and analyzed by immunoblotting (IB) for p-ERK5 and total ERK5. Normal rabbit immunoglobulin (normal IgG) was used as a negative control for immunoprecipitation. (C) Flow cytometric analysis. SNU449 cells were synchronized to the G1/S boundary using a double-thymidine block. Synchronized cells were released from the block and harvested at the indicated time points. The *X*-axis indicates DNA content and the *Y*-axis indicates the number of cells. (D) Time course of changes in the level of total ERK5 after release from the double-thymidine block. The level of β-actin was used as an internal control. (E) Time course of changes in the level of p-ERK5 after release from the double-thymidine block. ERK5 was immunoprecipitated from lysates of SNU449 cells harvested at the indicated times after release from the double-thymidine block. The samples were split and analyzed by immunoblotting for p-ERK5 and total ERK5. SNU449 cells, synchronized at the M phase with nocodazole, were also examined as described in (A) and (B). Normal rabbit IgG was used as a negative control for immunoprecipitation. (F) Representative images of mitotic cells in an SNU449 cell population that was transfected with *MAPK7*- or control-siRNA. SNU449 cells were treated with siRNA targeting *MAPK7*, negative control siRNA, or the transfection agent alone (Lipofectamine). Untreated cell were maintained under identical conditions. These cells were synchronized at the G1/S boundary using a double-thymidine block. The synchronized cells were released from the block and stained with anti-phospho-histone H3 9 hr after release, a time corresponding to the G2/M phase as shown in (C). Mitotic cells were identified by positive staining for phospho-histone H3 (green). Nuclear DNA was stained with propidium iodide (red). (G) The mitotic index was scored as described in Materials and Methods section. Data are presented as means ± SD (ANOVA; $^*P < 0.05$).

expression using RNAi and assessed its effect on mitosis. SNU449 cells were transfected with siRNA targeting *MAPK7* and synchronized at the G1/S-phase boundary by a double-thymidine block. The synchronized cells were released from the block and harvested 9 hr after release, a time which corresponds to the G2/M phase (Fig. 6C). Finally, harvested cells were stained with anti-phospho-histone H3 antibody, which specifically detects mitotic cells (Fig. 6F). Compared with a control siRNA or transfection agent alone, transfection of *MAPK7* siRNA significantly reduced the mitotic index (Fig. 6G). These findings suggest that ERK5 regulates mitotic entry in the HCC cells.

DISCUSSION

High-density SNP arrays are powerful tools for high-resolution analysis of DNA copy number aberrations in cancers. In the present study, using the Affymetrix GeneChip 100K and 250K SNP arrays we detected a novel amplification in HCC cells at 17p11. We were able to narrow the amplification to a 750-kb region. Notably, the amplification might have been missed using conventional analyses such as CGH. Amplification at 17p11.2-p12 has been detected in high-grade osteosarcoma using CGH (Forus et al., 1995; Tarkkanen et al., 1995). The group of van Dartel et al., (2002) established 17p11.2-p12 amplification profiles by semi-quantitative PCR using 15 microsatellite markers and seven candidate genes to assay amplification in this tumor type. They found that most of the tumors had complex amplification profiles, suggesting that multiple amplification targets, including *MAPK7*, might be present in region 17p11.2-p12. In contrast, we were able to define a smaller common region of amplification at 17p11 in two HCC cells and to determine the expression status of all genes in the amplicon. Three of the seven genes in the amplicon; *EPN2*, *EPPB9*, and *MAPK7*, were always overexpressed in cells that showed amplification in the 17p11 region. Thus, we considered these three genes as candidate targets for amplification. The function of *EPPB9* (B9 protein) is not known, and the protein encoded by *EPN2* (epsin 2) is similar to epsin 1, which plays a putative role in clathrin-mediated endocytosis (Rosenthal et al., 1999). Therefore, we focused on *MAPK7* as a target for the amplification.

Several lines of evidence implicate ERK5, which is encoded by *MAPK7*, in tumorigenesis (Wang and Tournier, 2006): (a) the ERK5 pathway is activated by Ras (English et al., 1999), ErbB (Esparis-Ogando et al., 2002; Yuste et al., 2005), Src (Sun et al., 2003), Cot (Chiariello et al., 2000), Bcr-Abl (Buschbeck et al., 2005), insulin-like growth factor-II (Linnerth et al., 2005), and interleukin-6 (Carvajal-Vergara et al., 2005); (b) ERK5 is involved in the control of breast cancer cell proliferation (Esparis-Ogando et al., 2002); (c) ERK5 mediates a survival signal that confers chemoresistance to breast cancer (Weldon et al., 2002); (d) insulin-like growth factor-II promotes cell survival via the ERK5 pathway in lung cancer cells (Linnerth et al., 2005); (e) the level of ERK5 contributes to the survival of Bcr/Abl-positive leukemic cells (Buschbeck et al., 2005); (f) ERK5 regulates cell proliferation and antiapoptotic responses in multiple myeloma (Carvajal-Vergara et al., 2005); and (g) an elevated level of MEK5, a specific activator of ERK5, is associated with metastasis and a poor prognosis in prostate cancer (Mehta et al., 2003).

The present study is the first to show the status of amplification and expression of *MAPK7* and its functional role in HCC. We found that *MAPK7* is amplified in 35 of 66 HCC tumors (53%). However, we could not determine the copy number of *MAPK7* in the nontumorous counterparts of the samples assayed because these samples were not available. Therefore, we cannot exclude the possibility that copy number polymorphism might influence the results of copy number analysis. We studied the expression of ERK5 using immunohistochemical analysis in primary HCCs and their surrounding nontumorous liver tissues. In nontumorous liver tissues, ERK5 was weakly expressed in the cytoplasm of non-neoplastic hepatocytes. Intriguingly, it was more strongly expressed in bile ducts, bile ductules, and a few small hepatocytes. In HCC tumor tissues, ERK5 was expressed in the cytoplasm of tumor cells. The level of ERK5 was elevated in 11 of 43 HCC tumors compared with their nontumorous counterparts. However, we did not observe a significant link between the level of ERK5 and any clinicopathological parameters. A recent report showed that, in prostate cancer, an increase in ERK5 cytoplasmic signals correlates with advanced disease and that strong nuclear ERK5 localization correlates with poor survival (McCracken et al., 2008).

We examined the functional roles of ERK5 in HCC cells using RNAi. Downregulation of *MAPK7* by siRNA suppressed the growth of

SNU449 cells, which had the greatest amplification and overexpression of *MAPK7* of all of the cell lines tested. These findings suggest that increased levels of ERK5 enhance the growth of HCC cells. Moreover, our results indicate that ERK5 is phosphorylated during the G2/M phases of the cell cycle and that it regulates entry into mitosis, which may explain how it promotes the growth of HCC cells.

Conflicting results have been reported by different investigators regarding the role of ERK5 in cell cycle progression. Some investigators have reported that ERK5 regulates the G1/S transition: expression of a dominant-negative form of ERK5 prevents cells from entering the S-phase of the cell cycle (Kato et al., 1998), and ERK5 can drive cyclin D1 expression (Mulloy et al., 2003). In contrast, Cude et al., (2007) and Gírio et al., (2007) recently reported that ERK5 is activated at the G2/M phases and is required for mitotic entry, findings that agree with our results.

Few molecules have been identified as direct downstream targets of ERK5. The transcriptional factors of the monocyte enhancer factor 2 family are among the best characterized substrates of ERK5. Phosphorylation of monocyte enhancer factor 2C by ERK5 enhances its transcriptional activity and subsequently leads to an increase in c-Jun gene expression (Kato et al., 1997; Wang and Tournier, 2006). A more complete identification of components downstream of ERK5 will be necessary to fully understand the role of ERK5 in carcinogenesis.

In summary, using high-density SNP arrays, we identified *MAPK7* as a probable target for the amplification events at 17p11 in HCCs. Our results suggest that the ERK5 protein product of the *MAPK7* gene plays a role in proliferation of HCC cells by regulating mitotic entry and may therefore be an optimal target for the development of novel therapies for this widespread type of cancer.

REFERENCES

Aden DP, Fogel A, Plotkin S, Damjanov I, Knowles BB. 1979. Controlled synthesis of HBsAg in a differentiated human liver carcinoma-derived cell line. Nature 282:615–616.

Alexander JJ, Bey EM, Geddes EW, Lecatsas G. 1976. Establishment of a continuously growing cell line from primary carcinoma of the liver. S Afr Med J 50:2124–2128.

Bignell GR, Huang J, Greshock J, Watt S, Butler A, West S, Grigorova M, Jones KW, Wei W, Stratton MR, Futreal PA, Weber B, Shapero MH, Wooster R. 2004. High-resolution analysis of DNA copy number using oligonucleotide microarrays. Genome Res 14:287–295.

Buschbeck M, Hofbauer S, Di Croce L, Keri G, Ullrich A. 2005. Abl-kinase-sensitive levels of ERK5 and its intrinsic basal activity contribute to leukaemia cell survival. EMBO Rep 6:63–69.

Carvajal-Vergara X, Tabera S, Montero JC, Esparís-Ogando A, López-Pérez R, Mateo G, Gutiérrez N, Parmo-Cabañas M, Teixidó J, San Miguel JF, Pandiella A. 2005. Multifunctional role of Erk5 in multiple myeloma. Blood 105:4492–4499.

Chiariello M, Marinissen MJ, Gutkind JS. 2000. Multiple mitogen-activated protein kinase signaling pathways connect the cot oncoprotein to the c-jun promoter and to cellular transformation. Mol Cell Biol 20:1747–1758.

Collins C, Rommens JM, Kowbel D, Godfrey T, Tanner M, Hwang SI, Polikoff D, Nonet G, Cochran J, Myambo K, Jay KE, Froula J, Cloutier T, Kuo WL, Yaswen P, Dairkee S, Giovanola J, Hutchinson GB, Isola J, Kallioniemi OP, Palazzolo M, Martin C, Ericsson C, Pinkel D, Albertson D, Li WB, Gray JW. 1998. Positional cloning of ZNF217 and NABC1: Genes amplified at 20q13.2 and overexpressed in breast carcinoma. Proc Natl Acad Sci USA 95:8703–8708.

Cude K, Wang Y, Choi HJ, Hsuan SL, Zhang H, Wang CY, Xia Z. 2007. Regulation of the G2-M cell cycle progression by the ERK5-NFkappaB signaling pathway. J Cell Biol 177:253–264.

Di Fiore PP, Pierce JH, Kraus MH, Segatto O, King CR, Aaronson SA. 1987. erbB-2 is a potent oncogene when overexpressed in NIH/3T3 cells. Science 237:178–182.

Di X, Matsuzaki H, Webster TA, Hubbell E, Liu G, Dong S, Bartell D, Huang J, Chiles R, Yang G, Shen MM, Kulp D, Kennedy GC, Mei R, Jones KW, Cawley S. 2005. Dynamic model based algorithms for screening and genotyping over 100 K SNPs on oligonucleotide microarrays. Bioinformatics 21:1958–1963.

Dor I, Namba M, Sato J. 1975. Establishment and some biological characteristics of human hepatoma cell lines. Gann 66:385–392.

El-Serag HB. 2002. Hepatocellular carcinoma: An epidemiologic view. J Clin Gastroenterol 35:S72–S78.

English JM, Pearson G, Hockenberry T, Shivakumar L, White MA, Cobb MH. 1999. Contribution of the ERK5/MEK5 pathway to Ras/Raf signaling and growth control. J Biol Chem 274:31588–1592.

Esparis-Ogando A, Diaz-Rodriguez E, Montero JC, Yuste L, Crespo P, Pandiella A. 2002. Erk5 participates in neuregulin signal transduction and is constitutively active in breast cancer cells overexpressing ErbB2. Mol Cell Biol 22:270–285.

Forus A, Weghuis DO, Smeets D, Fodstad O, Myklebost O, Geurts van Kessel A. 1995. Comparative genomic hybridization analysis of human sarcomas. II. Identification of novel amplicons at 6p and 17p in osteosarcomas. Genes Chromosomes Cancer 14:15–21.

Fujise K, Nagamori S, Hasumura S, Homma S, Sujino H, Matsuura T, Shimizu K, Niiya M, Kameda H, Fujita K. 1990. Integration of hepatitis B virus DNA into cells of six established human hepatocellular carcinoma cell lines. Hepatogastroenterology 37:457–460.

Garaude J, Cherni S, Kaminski S, Delepine E, Chable-Bessia C, Benkirane M, Borges J, Pandiella A, Iñiguez MA, Fresno M, Hipskind RA, Villalba M. 2006. ERK5 activates NF-kappaB in leukemic T cells and is essential for their growth in vivo. J Immunol 177:7607–7617.

Garraway LA, Widlund HR, Rubin MA, Getz G, Berger AJ, Ramaswamy S, Beroukhim R, Milner DA, Granter SR, Du J, Lee C, Wagner SN, Li C, Golub TR, Rimm DL, Meyerson ML, Fisher DE, Sellers WR. 2005. Integrative genomic analyses identify MITF as a lineage survival oncogene amplified in malignant melanoma. Nature 436:117–122.

Gírio A, Montero JC, Pandiella A, Chatterjee S. 2007. Erk5 is activated and acts as a survival factor in mitosis. Cell Signal 19:1964–1972.

Hayashi M, Lee JD. 2004. Role of the BMK1/ERK5 signaling pathway: Lessons from knockout mice. J Mol Med 82:800–808.

Hirohashi S, Shimosato Y, Kameya T, Koide T, Mukojima T, Taguchi Y, Kageyama K. 1979. Production of -fetoprotein and normal serum proteins by xenotransplanted human hepatomas in relation to their growth and morphology. Cancer Res 39: 1819–1828.

Huh N, Utakoji T. 1981. Production of HBs-antigen by two new human hepatoma cell lines and its enhancement by dexamethasone. Gann 72:178–179.

Kallioniemi A, Kallioniemi OP, Sudar D, Rutovitz D, Gray JW, Waldman F, Pinkel D. 1992. Comparative genomic hybridization for molecular cytogenetic analysis of solid tumors. Science 258:818–821.

Kato Y, Kravchenko VV, Tapping RI, Han J, Ulevitch RJ, Lee JD. 1997. BMK1/ERK5 regulates serum-induced early gene expression through transcription factor MEF2C. EMBO J 16:7054–7066.

Kato Y, Tapping RI, Huang S, Watson MH, Ulevitch RJ, Lee JD. 1998. Bmk1/Erk5 is required for cell proliferation induced by epidermal growth factor. Nature 395:713–716.

Kennedy GC, Matsuzaki H, Dong S, Liu WM, Huang J, Liu G, Su X, Cao M, Chen W, Zhang J, Liu W, Yang G, Di X, Ryder T, He Z, Surti U, Phillips MS, Boyce-Jacino MT, Fodor SP, Jones KW. 2003. Large-scale genotyping of complex DNA. Nat Biotechnol 21:1233–1237.

Knowles BB, Howe CC, Aden DP. 1980. Human hepatocellular carcinoma cell lines secrete the major plasma proteins and hepatitis B surface antigen. Science 209:97–499.

Linnerth NM, Baldwin M, Campbell C, Brown M, McGowan H, Moorehead RA. 2005. IGF-II induces CREB phosphorylation and cell survival in human lung cancer cells. Oncogene 24:7310–7319.

Little CD, Nau MM, Carney DN, Gazdar AF, Minna JD. 1983. Amplification and expression of the c-myc oncogene in human lung cancer cell lines. Nature 306:194–196.

Matsuzaki H, Dong S, Loi H, Di X, Liu G, Hubbell E, Law J, Berntsen T, Chadha M, Hui H, Yang G, Kennedy GC, Webster TA, Cawley S, Walsh PS, Jones KW, Fodor SP, Mei R. 2004a. Genotyping over 100,000 SNPs on a pair of oligonucleotide arrays. Nat Methods 1:109–111.

Matsuzaki H, Loi H, Dong S, Tsai YY, Fang J, Law J, Di X, Liu WM, Yang G, Liu G, Huang J, Kennedy GC, Ryder TB, Marcus GA, Walsh PS, Shriver MD, Puck JM, Jones KW, Mei R. 2004b. Parallel genotyping of over 10,000 SNPs using a one-primer assay on a high-density oligonucleotide array. Genome Res 14:414–425.

McCracken SR, Ramsay A, Heer R, Mathers ME, Jenkins BL, Edwards J, Robson CN, Marquez R, Cohen P, Leung HY. 2008. Aberrant expression of extracellular signal-regulated kinase 5 in human prostate cancer. Oncogene 27:2978–2988.

Mehta PB, Jenkins BL, McCarthy L, Thilak L, Robson CN, Neal DE, Leung HY. 2003. MEK5 overexpression is associated with metastatic prostate cancer, and stimulates proliferation, MMP-9 expression and invasion. Oncogene 22:1381–1389.

Mei R, Galipeau PC, Prass C, Berno A, Ghandour G, Patil N, Wolff RK, Chee MS, Reid BJ, Lockhart DJ. 2000. Genome-wide detection of allelic imbalance using human SNPs and high-density DNA arrays. Genome Res 10:1126–1137.

Minamiya Y, Matsuzaki I, Sageshima M, Saito H, Taguchi K, Nakagawa T, Ogawa J. 2004. Expression of tissue factor mRNA and invasion of blood vessels by tumor cells in non-small cell lung cancer. Surg Today 34:1–5.

Mulloy R, Salinas S, Philips A, Hipskind RA. 2003. Activation of cyclin D1 expression by the ERK5 cascade. Oncogene 22:5387–5398.

Nakabayashi H, Taketa K, Miyano K, Yamane T, Sato J. 1982. Growth of human hepatoma cells lines with differentiated functions in chemically defined medium. Cancer Res 42:3858–3863.

Nannya Y, Sanada M, Nakazaki K, Hosoya N, Wang L, Hangaishi A, Kurokawa M, Chiba S, Bailey DK, Kennedy GC, Ogawa S. 2005. A robust algorithm for copy number detection using high-density oligonucleotide single nucleotide polymorphism genotyping arrays. Cancer Res 65:6071–6079.

Nishimoto S, Nishida E. 2006. MAPK signalling: ERK5 versus ERK1/2. EMBO Rep 7:782–786.

Okamoto H, Yasui K, Zhao C, Arii S, Inazawa J. 2003. PTK2 and EIF3S3 genes may be amplification targets at 8q23-q24 and are associated with large hepatocellular carcinomas. Hepatology 38:1242–1249.

Park JG, Lee JH, Kang MS, Park KJ, Jeon YM, Lee HJ, Kwon HS, Park HS, Yeo KS, Lee KU, Kim ST, Chung JK, Hwang YJ, Lee HS, Kim CY, Lee YI, Chen TR, Hay RJ, Song SY, Kim WH, Kim CW, Kim YI. 1995. Characterization of cell lines established from human hepatocellular carcinoma. Int J Cancer 62:276–282.

Rosenthal JA, Chen H, Slepnev VI, Pellegrini L, Salcini AE, Di Fiore PP, De Camilli P. 1999. The epsins define a family of proteins that interact with components of the clathrin coat and contain a new protein module. J Biol Chem 274:33959–33965.

Sun W, Wei X, Kesavan K, Garrington TP, Fan R, Mei J, Anderson SM, Gelfand EW, Johnson GL. 2003. MEK kinase 2 and the adaptor protein Lad regulate extracellular signal-regulated kinase 5 activation by epidermal growth factor via Src. Mol Cell Biol 23:2298–2308.

Tarkkanen M, Karhu R, Kallioniemi A, Elomaa I, Kivioja AH, Nevalainen J, Böhling T, Karaharju E, Hyytinen E, Knuutila S, Kallioniemi OP. 1995. Gains and losses of DNA sequences in osteosarcomas by comparative genomic hybridization. Cancer Res 55:1334–1338.

van Dartel M, Cornelissen PW, Redeker S, Tarkkanen M, Knuutila S, Hogendoorn PC, Westerveld A, Gomes I, Bras J, Hulsebos TJ. 2002. Amplification of 17p11.2 approximately p12, including PMP22, TOP3A, and MAPK7, in high-grade osteosarcoma. Cancer Genet Cytogenet 139:91–96.

Wang X, Tournier C. 2006. Regulation of cellular functions by the ERK5 signalling pathway. Cell Signal 18:753–760.

Weldon CB, Scandurro AB, Rolfe KW, Clayton JL, Elliott S, Butler NN, Melnik LI, Alam J, McLachlan JA, Jaffe BM, Beckman BS, Burow ME. 2002. Identification of mitogen-activated protein kinase kinase as a chemoresistant pathway in MCF-7 cells by using gene expression microarray. Surgery 132:293–301.

Wong KK, Tsang YT, Shen J, Cheng RS, Chang YM, Man TK, Lau CC. 2004. Allelic imbalance analysis by high-density single-nucleotide polymorphic allele (SNP) array with whole genome amplified DNA. Nucleic Acids Res 32:e69.

Yasui K, Arii S, Zhao C, Imoto I, Ueda M, Nagai H, Emi M, Inazawa J. 2002. TFDP1, CUL4A, and CDC16 identified as targets for amplification at 13q34 in hepatocellular carcinomas. Hepatology 35:1476–1484.

Yasui K, Imoto I, Fukuda Y, Pimkhaokham A, Yang ZQ, Naruto T, Shimada Y, Nakamura Y, Inazawa J. 2001. Identification of target genes within an amplicon at 14q12-q13 in esophageal squamous cell carcinoma. Genes Chromosomes Cancer 32:112–118.

Yokoi S, Yasui K, Iizasa T, Imoto I, Fujisawa T, Inazawa J. 2003. TERC identified as a probable target within the 3q26 amplicon that is detected frequently in non-small cell lung cancers. Clin Cancer Res 9:4705–4713.

Yokoi S, Yasui K, Saito-Ohara F, Koshikawa K, Iizasa T, Fujisawa T, Terasaki T, Horii A, Takahashi T, Hirohashi S, Inazawa J. 2002. A novel target gene, SKP2, within the 5p13 amplicon that is frequently detected in small cell lung cancers. Am J Pathol 161:207–216.

Yuste L, Montero JC, Esparis-Ogando A, Pandiella A. 2005. Activation of ErbB2 by overexpression or by transmembrane neuregulin results in differential signaling and sensitivity to herceptin. Cancer Res 65:6801–6810.

Zhao X, Li C, Paez JG, Chin K, Jänne PA, Chen TH, Girard L, Minna J, Christiani D, Leo C, Gray JW, Sellers WR, Meyerson M. 2004. An integrated view of copy number and allelic alterations in the cancer genome using single nucleotide polymorphism arrays. Cancer Res 64:3060–3071.

Zhao X, Weir BA, LaFramboise T, Lin M, Beroukhim R, Garraway L, Beheshti J, Lee JC, Naoki K, Richards WG, Sugarbaker D, Chen F, Rubin MA, Jänne PA, Girard L, Minna J, Christiani D, Li C, Sellers WR, Meyerson M. 2005. Homozygous deletions and chromosome amplifications in human lung carcinomas revealed by single nucleotide polymorphism array analysis. Cancer Res 65:5561–5570.

Association of Gankyrin Protein Expression with Early Clinical Stages and Insulin-Like Growth Factor-Binding Protein 5 Expression in Human Hepatocellular Carcinoma

Atsushi Umemura,[1,2] Yoshito Itoh,[2] Katsuhiko Itoh,[1] Kanji Yamaguchi,[2] Tomoki Nakajima,[2] Hiroaki Higashitsuji,[1] Hitoshi Onoue,[3] Manabu Fukumoto,[4] Takeshi Okanoue,[2] and Jun Fujita[1]

Gankyrin (also known as PSMD10) is a liver oncoprotein that interacts with multiple proteins including MDM2 and accelerates degradation of the tumor suppressors p53 and Rb. We produced a monoclonal anti-gankyrin antibody and immunohistochemically assessed the clinicopathological significance of gankyrin overexpression in 43 specimens of human hepatocellular carcinoma (HCC). Specific cytoplasmic staining for gankyrin was observed in 62.8% (27/43) of HCCs, which was significantly associated with low TNM stage ($P = 0.004$), no capsular invasion ($P = 0.018$), no portal venous invasion ($P = 0.008$), and no intrahepatic metastasis ($P = 0.012$). The cumulative survival rate of patients with gankyrin-positive HCC was significantly higher than that with gankyrin-negative HCC ($P = 0.037$). p53 and MDM2 were positively stained by antibodies in 30.2% and 23.3%, respectively, of HCCs, but neither was inversely associated with gankyrin expression. In the Huh-7 human HCC cell line, overexpression of gankyrin up-regulated expression of insulin-like growth factor binding protein 5 (IGFBP-5), whereas suppression of gankyrin expression by siRNA down-regulated it. Supression of IGFBP-5 expression inhibited proliferation of Huh-7 cells as well as U-2 OS osteosarcoma cells. In HCC specimens, positive staining for IGFBP-5 was observed by immunohistochemistry in 41.9% (18/43), and the level of expression was significantly correlated with that of gankyrin (*rho* = 0.629, $P < 0.001$). *Conclusion:* These results suggest that gankyrin plays an oncogenic role(s) mainly at the early stages of human hepatocarcinogenesis, and that IGFBP-5 inducible by gankyrin overexpression may be involved in it. (HEPATOLOGY 2008;47:493-502.)

Liver cancer is the sixth most common cancer worldwide (626,000 or 5.7% of new cancer cases) and the third most common cause of death from cancer (598,000) in 2002.[1] Eighty-two percent of cases are in developing countries, and the areas of high incidence are sub-Saharan Africa, eastern and southeastern Asia, and Melanesia. Histologically, more than 90% of the primary liver cancers are hepatocellular carcinomas (HCCs). Although there are several modalities of treatment for HCC, most patients present with unresectable tumors, and nonsurgical treatments are minimally effective at best.[2,3] Even for those patients who undergo surgical resection, the recurrence rate is very high and the prognosis is poor.[2,4-6] It is therefore important to clarify the mechanisms of human hepatocarcinogenesis and identify molecular targets to develop novel diagnostic, therapeutic, and preventive strategies.

By constructing subtracted complementary DNA (cDNA) libraries, we have previously identified 19 genes overexpressed in HCCs including 2 novel genes.[7,8] One of them was named gankyrin (gann-ankyrin repeat pro-

Abbreviations: 3A6C2, mouse monoclonal anti-gankyrin antibody; cDNA, complementary DNA; HCC, hepatocellular carcinoma; IGF, insulinlike growth factor; IGFBP-5, insulin-like growth factor-binding protein 5; MDM2, mouse double minute 2; mRNA, messenger RNA; RT-PCR, reverse transcription polymerase chain reaction; siRNA, short interfering RNA; TNM, tumor-node-metastasis.

From the [1]Department of Clinical Molecular Biology, Graduate School of Medicine, Kyoto University, Kyoto, Japan; the [2]Molecular Gastroenterology and Hepatology, Graduate School of Medical Science, Kyoto Prefectural University of Medicine, Kyoto, Japan; the [3]Department of Nutritional Science, Faculty of Health and Welfare, Seinan Jo Gakuin University, Kitakyushu, Japan; and the [4]Department of Pathology, Institute of Development, Aging, and Cancer, Tohoku University, Sendai, Japan

Received May 21, 2007; accepted September 3, 2007.

Supported by Grants-in aid from the Ministry of Education, Culture, Sports, Science, and Technology of Japan and the Japan Society for the Promotion of Science.

Address reprint requests to: Jun Fujita, Department of Clinical Molecular Biology, Graduate School of Medicine, Kyoto University, 54 Shogoin Kawaharacho, Sakyo-ku, Kyoto 606-8507, Japan. E-mail: jfujita@virus.kyoto-u.ac.jp; fax: (81) 75-751-4977.

Published online in Wiley InterScience (www.interscience.wiley.com).

DOI 10.1002/hep.22027

Potential conflict of interest: Nothing to report.

tein; "gann" in Japanese means cancer).[9] Gankyrin (also called PSMD10) consists of 7 ankyrin repeats, and its messenger RNA (mRNA) was overexpressed in 34 of 34 HCCs analyzed.[9,10] Independently, gankyrin was isolated as the p28 component or the interactor of the S6b subunit of the 19S regulator of the 26S proteasome.[11,12] The ankyrin repeat is the functional domain involved in protein–protein interactions, and gankyrin has been shown to interact with multiple proteins in addition to S6b. Gankyrin binds to retinoblastoma protein (Rb) and cyclin-dependent kinase (Cdk4), and accelerates phosphorylation and degradation of Rb, which results in release of the E2F transcription factor to activate DNA synthesis genes.[9,13] Gankyrin seems to play a role in cell cycle progression in noncancerous cells as well. Overexpression of gankyrin shortens population doubling time of NIH/3T3 mouse fibroblasts,[9] and its up-regulation correlates with cell cycle progression in normal rat primary hepatocytes, oval cells, and human hepatocytes.[14,15]

Overexpression of gankyrin confers tumorigenicity to NIH/3T3 cells and inhibits apoptosis in cultured human tumor cells exposed to chemotherapeutic agents.[10] The anti-apoptotic activity is attributable, at least partly, to increased degradation of p53, resulting in the reduced transcription of the p53-dependent proapoptotic genes.[16] Gankyrin binds to the E3 ubiquitin ligase MDM2 *in vitro* and *in vivo*, which increases p53–MDM2 association, thereby facilitating the ubiquitination and subsequent proteasomal degradation of p53 by MDM2. Gankyrin also controls MDM2 auto-ubiquitination and degradation, especially in the absence of p53.[16]

We produced a mouse monoclonal antibody against human gankyrin and assessed the expression of gankyrin protein in surgically resected HCC specimens by immunohistochemistry. Correlation of gankyrin positivity with clinicopathological findings and expression of p53 and MDM2 in HCC was analyzed. Furthermore, we demonstrated that expression of insulin-like growth factor-binding protein 5 (IGFBP-5) is inducible by overexpression of gankyrin in HCCs.

Patients and Methods

Patients and Specimens. HCC tissues and their corresponding noncancerous liver tissues were obtained from 43 and 32 patients, respectively, who had undergone curative hepatectomy at the University Hospital of Kyoto Prefectural University of Medicine between 1992 and 2000. The specimens used were routinely processed, formalin-fixed, and paraffin-embedded. After hematoxylin-eosin staining, all samples were diagnosed as HCC and the tumor-node-metastasis (TNM) classification was made according to the fourth edition of the general rules for the clinical and pathological study of primary liver cancer proposed by the Liver Cancer Study Group of Japan.[17] The demographic profiles of the patients are summarized in Table 1. For western blot analysis, HCCs and noncancerous liver tissues were obtained from 3 patients undergoing liver transplantation at the University Hospital of Kyoto Prefectural University of Medicine between 2004 and 2006. No donor organs were obtained from executed prisoners or other institutionalized persons. The study protocol conformed to the ethical guidelines of the 1975 Declaration of Helsinki and was approved by the institutional review boards. Written informed consents were obtained from all patients for subsequent use of their resected tissues.

Table 1. Patient and Tumor Characteristics

Characteristic	Number (Percentage)
Number of patients	43
Sex distribution	
Male	27 (62.8%)
Female	16 (37.2%)
Age (years)	25-78, median 65
Virus marker	
HBV(+)/HCV(−)	6 (14.0%)
HBV(−)/HCV(+)	28 (65.0%)
HBV(+)/HCV(+)	3 (7.0%)
HBV(−)/HCV(−)	6 (14.0%)
AFP(ng/mL)	3.5-39999, median 90
Tumor size (cm)	1.6-17.0, median 4.0
Liver cirrhosis	
Yes	29 (67.5%)
No	14 (32.5%)
Chronic hepatitis	13 (30.2%)
Normal	1 (2.3%)
TNM stage	
I	4 (9.3%)
II	22 (51.1%)
III	8 (18.6%)
IV	9 (21.0%)
Histological differentiation	
Well	12 (27.9%)
Moderate	25 (58.1%)
Poor	6 (14.0%)
Capsular formation	
Yes	36 (83.7%)
No	7 (16.3%)
Capsular invasion	
Yes	14 (32.6%)
No	29 (67.4%)
Portal venous invasion	
Yes	9 (20.9%)
No	34 (79.1%)
Intrahepatic metastasis	
Yes	16 (37.2%)
No	27 (62.8%)

Abbreviations: HCV(+), anti-hepatitis C virus antibody positive; HBV(+), hepatitis B surface antigen positive; (−), negative; AFP, serum alpha-fetoprotein.